Transcription of a plasticity gene is activated by neuronal hyperpolarization

Zhonghua Zhu[1], Tamara Sanchez Ortiz[1], Shaul Mezan[2], Sebastian Kadener[2,3] & Justin Blau[1, 4, 5 *]

[1] Department of Biology, New York University, 100 Washington Square East, New York, NY 10003, USA

[2] Biological Chemistry Department, Silberman Institute of Life Sciences, The Hebrew University of Jerusalem, Jerusalem, 91904, Israel

[3] Biology Department, Brandeis University, Waltham, MA, 02454, USA

[4] Center for Genomics & Systems Biology, New York University Abu Dhabi Institute, Abu Dhabi, United Arab Emirates

[5] Lead contact

[*] Correspondence: justin.blau@nyu.edu

Running title: A gene expression program activated by neuronal inactivity

Summary

Long term synaptic plasticity requires transcription in response to changes in neuronal activity. While genes induced by neuronal activity have been extensively studied, genes induced by hyperpolarization are largely unknown. We focused on *Pura*, a Rho1 GEF whose rhythmic expression drives the daily retraction of the projections of *Drosophila* LN_v circadian pacemaker neurons. We found that *Pura* transcription is repressed by activity and induced by hyperpolarization in LN_vs – the opposite of typical activity-regulated genes. *Pura* is repressed by activity-regulated transcriptional factors including Mef2 and Sr (fly Egr-1) and activated by Toy, a Pax6 transcription factor. *toy* transcription is also induced by inactivity. Thus *toy* and *Pura* represent a class of genes induced by hyperpolarization.

Highlights

- Hyperpolarization activates transcription of *Pura*, a plasticity gene
- This phenomenon occurs in circadian pacemaker neurons and mushroom body neurons
- The *Pura* enhancer integrates recent neuronal activity to regulate transcription
- Hyperpolarization activates transcription of *toy* (Pax-6), which then activates *Pura*

Introduction

Neuronal plasticity is essential for the nervous system to wire correctly and underlies processes including learning and memory and recovery from strokes (reviewed by (Kandel et al., 2014; Murphy and Corbett, 2009). Disruptions to plasticity are increasingly being associated with neurological disorders such as autism spectrum disorder and schizophrenia (reviewed by (Ebert and Greenberg, 2013; Glausier and Lewis, 2013).

Plasticity encompasses changes in both the excitability and structure of neurons. While changes in neuronal excitability alter the strength of the signals transmitted, structural plasticity can make new connections between neurons. New gene expression plays a major role in plasticity via a set of activity-dependent genes whose transcription is rapidly induced by neuronal firing. The products of activity-dependent genes such as *Arc* and *Homer1a* directly regulate synaptic function (reviewed by (Leslie and Nedivi, 2011), while others such as *c-fos* and *Nur77* / *Nr4a1* encode transcription factors whose targets likely include genes that alter neuronal connectivity (Yang et al., 2016).

However, neuronal plasticity also includes reducing neuronal excitability and weakening or losing connections. These aspects of neuronal plasticity are probably important in forgetting memories and also in sleep, in which widespread synaptic downscaling has been proposed to reduce overall connectivity in the brain (de Vivo et al., 2017; Diering et al., 2017). However, relatively few molecular mechanisms have so far been described to explain how neurons decrease their connectivity and the role of gene expression in this phenomenon has been largely ignored.

One example of how gene expression can weaken neuronal connections comes from *Drosophila* circadian pacemaker neurons, which drive ~24hr rhythms in behavior. A subset of pacemaker neurons – the 4 small ventral lateral neurons (s-LN_vs) in each brain hemisphere – show predictable and intrinsic daily rhythms in their excitability (Cao and Nitabach, 2008) and in the structure of their projections (Cao and Nitabach, 2008; Fernandez et al., 2008). We recently showed that Rho1 activity is rhythmic in s-LN_v projections and this is regulated by rhythmic expression of *Puratrophin-like* (*Pura*), a Rho1 Guanine nucleotide exchange factor (GEF) that increases Rho1 activity (Petsakou et al., 2015).

s-LN_v plasticity is also regulated by neuronal activity, which normally peaks around dawn (Cao and Nitabach, 2008) when s-LN_v projections are maximally expanded. (Sivachenko et al., 2013) found that artificially inducing s-LN_vs to fire at dusk rapidly expanded their projections to the dawn-like state. Part of the mechanism that allows s-LN_v projections to expand at dusk in response to firing could be that increasing neuronal activity reduces *Pura* RNA levels in LN_vs (Chen et al., 2016; Mizrak et al., 2012). Indeed, it seems important for neuronal activity to repress genes such as *Pura* that retract neuronal projections since activity-induced genes tend to have the opposite effect to *Pura* on neuronal structure (Yang et al., 2016).

We investigated how *Pura* transcription responds to neuronal activity. We constructed transcriptional reporter genes for *Pura* and *Hr38*, which is a typical activity-regulated gene: *Hr38* expression is induced by neuronal activity in invertebrates just like its mammalian orthologue *Nr4a1* (Fujita et al., 2013; Milbrandt, 1988). Neuronal activity induced *Hr38* but repressed *Pura* transcription in LN_v clock neurons. More interestingly, hyperpolarizing LN_vs activated *Pura* transcription and repressed *Hr38* transcription. Thus transcription of *Hr38* and *Pura* responds to both neuronal activity and hyperpolarization, but in opposite directions to each other.

Dissecting the *Pura* regulatory region, we identified an 116bp enhancer that gives the correct spatial and temporal expression of *Pura* in LN_vs as well as responding to both neuronal activity and hyperpolarization. This enhancer contains binding sites for Mef2, Stripe (Sr, the *Drosophila* Egr-1 orthologue) and Atf-3, which are either post-translationally or transcriptionally activated by neuronal activity in mammals (Mao et al., 1999; Milbrandt, 1987; Zhang et al., 2011). All three factors repressed *Pura* transcription, suggesting a mechanism for how neuronal activity represses *Pura*. We also identified that Toy, one of the two *Drosophila* Pax6 transcription factors (Czerny et al., 1999), activates *Pura* transcription likely through a Toy binding site in the minimal *Pura* enhancer. Since the Toy binding site in the minimal *Pura* enhancer overlaps the Mef2 and Sr binding sites, the *Pura* enhancer seems to integrate recent neuronal activity to determine levels of *Pura* transcription. Strikingly, *toy* transcription itself is activated when LN_vs are hyperpolarized. We propose that inactivity-driven gene expression is a general property of plastic neurons.

Results

Transcription of *Hr38* and *Pura* responds in opposite directions to neuronal activity and hyperpolarization

We developed reporter genes to test if transcription of *Hr38* and *Pura* responds to neuronal activity. To identify the regulatory regions that direct expression to LN_vs, we crossed the available *Hr38-* and *Pura-Gal4* lines (Jenett et al., 2012; Kvon et al., 2014) to *UAS-GFP* and identified one Gal4 line for each gene that expressed in larval LN_vs (Fig. 1A and Fig. S1A). The *Hr38* enhancer from this Gal4 line was fused upstream of the *Hsp70* basal promoter, whereas the *Pura* enhancer already contained its endogenous basal promoter and transcriptional start site. Downstream we fused a codon-optimized and destabilized tdTomato fluorescent protein, which has three copies of a nuclear localization signal (NLS) to focus signals for quantification (Mezan et al., 2016). We also added an intervening sequence (IVS) to promote nuclear export of spliced mRNA (Pfeiffer et al., 2010) and a synthetic 5' UTR (Syn21) to increase translation (Pfeiffer et al., 2012). *Hr38-* and *Pura-Tomato* constructs were inserted to the same location as each other on chromosome 2.

To test if the reporter genes follow the temporal patterns of *Hr38* and *Pura* RNA, we measured Tomato levels in larval LN_vs across a 12hr:12hr light:dark (LD) cycle. We found that *Hr38-Tomato* levels in LN_vs peak at ZT2 (Zeitgeber Time, ZT0 = lights on, ZT12 = lights off) (Fig. 1B). This is consistent with previous reports of higher *Hr38* mRNA levels in LN_vs at CT3 than CT15 (Circadian Time, time in constant darkness after entrainment in LD cycles) (Mizrak et al., 2012) and with LN_vs being more excitable at dawn than dusk (Cao and Nitabach, 2008). *Pura-Tomato* levels were maximal at ZT18 and low by ZT24 (Fig. 1B), which is very similar to *Pura* RNA (Ruben et al., 2012). The data shown here are for *Pura-Tomato B*, which has ~1.5kb of regulatory region directly upstream of the *Pura* basal promoter. *Pura-Tomato B* showed very similar temporal dynamics as *Pura-Tomato A*, which has an additional ~0.5kb downstream of the transcriptional start site (Fig. S1B). Thus the *Hr38* and *Pura* transcriptional reporters have similar temporal dynamics to their RNAs (Mizrak et al., 2012; Ruben et al., 2012).

To test how neuronal activity regulates *Hr38* and *Pura* transcription, we first used a *UAS-NaChBac* transgene (*UAS-NCB*) to hyperexcite LN_vs. *NCB* is a low threshold voltage-gated bacterial Na^+ channel that increases LN_v excitability (Nitabach et al., 2006; Yuan

et al., 2011). *UAS-NCB* was expressed specifically in larval LN_vs using a *Pigment dispersing factor-Gal4* driver (*Pdf-Gal4*) (Park et al., 2000). [In the figures, we use the nomenclature *Pdf > X* to indicate larvae with *Pdf-Gal4* and *UAS-X* transgenes.] Larvae were entrained in LD and *Hr38-* and *Pura-Tomato* levels were measured at ZT24, just before the normal increase in *Hr38* transcription after dawn. Expressing NCB in LN_vs increased *Hr38-Tomato* levels 2.2-fold and reduced *Pura-Tomato* levels 1.4-fold compared to control LN_vs expressing a *UAS-GFP* transgene (Fig. 1C).

To test how hyperpolarization affects *Hr38* and *Pura* transcription, we used *Pdf-Gal4* to express *UAS-Kir2.1*, a mammalian inward rectifier K^+ channel (Baines et al., 2001). We again measured *Hr38-* and *Pura-Tomato* levels at ZT24 and found that *Hr38-Tomato* levels were 2-fold lower while *Pura-Tomato* levels were 3.3-fold higher in Kir2.1-expressing LN_vs than in control LN_vs (Fig. 1C). Thus transcription of *Hr38* and *Pura* responds in opposite directions to long-term changes in neuronal activity: *Hr38* transcription is activated when LN_vs are hyperexcited and repressed when LN_vs are hyperpolarized, whereas *Pura* is activated by hyperpolarization and repressed by increased activity.

***Hr38* and *Pura* transcription responds in opposite directions to transient changes in neuronal activity**

To test if *Hr38* and *Pura* transcription respond to more transient changes in neuronal activity, we used *Pdf-Gal4* to ectopically express *UAS-dTrpA1*, a heat-activated *Drosophila* cation channel (Hamada et al., 2008). Since TrpA1 is inactive below 23°C, larvae were entrained in LD cycles at 22°C and then shifted to 30°C for 4hr from ZT12 to ZT16. We selected lights-off to induce firing since LN_vs are normally relatively inactive at this time (Cao and Nitabach, 2008). The data in Fig. 2A show that *Hr38-Tomato* levels at ZT16 were 3.8-fold higher in *dTrpA1*-expressing LN_vs than in control LN_vs without a *dTrpA1* transgene that followed the same temperature shift. In contrast, *Pura-Tomato* levels were 4.6-fold lower in *dTrpA1*-expressing LN_vs than in control LN_vs.

We also tested the responses of *Hr38* and *Pura* to transient hyperpolarization. For this, we used a temperature-sensitive Gal80 transgene (*tubulin-Gal80^{ts}*, (McGuire et al., 2003)) to repress Gal4 activity and regulate expression of *UAS-Kir2.1*. Larvae were entrained in LD cycles at 18°C when $Gal80^{ts}$ is active and shifted to 30°C at ZT22 to

inactivate Gal80 and induce *Kir2.1* expression. Larvae were maintained at 30°C for 4hr in darkness to prevent light-induced neuronal activity (Yuan et al., 2011). The data in Fig. 2B show that *Hr38-Tomato* levels were 1.4-fold lower while *Pura-Tomato* levels were 2-fold higher in LN_vs expressing *Kir2.1* than in control LN_vs. Thus *Hr38* and *Pura* transcription respond in the same way to more transient changes in LN_v electrical activity (Fig. 2A, B) as they do to long-term changes (Fig. 1C).

_Hr38_ and _Pura_ transcription respond in opposite directions to hyperpolarization via an intact neural circuit

The DN1 dorsal larval clock neurons release glutamate and inhibit LN_vs via GluCl, a glutamate-gated chloride channel (Collins et al., 2012). We therefore decided to manipulate DN1 activity and ask if changes in *Hr38* and *Pura* transcription in LN_vs could be detected when LN_v activity was altered via an inhibitory neural circuit.

cry39-Gal4 was used with *Pdf-Gal80* to restrict *UAS-dTrpA1* and *UAS-GFP* expression to larval DN1s. *cry39-Gal4* is expressed in larval DN1s and LN_vs (Picot et al., 2007), but the temperature-independent *Pdf-Gal80* transgene (Stoleru et al., 2004) constitutively blocks Gal4 activity in LN_vs. We confirmed this by assaying GFP localization (Fig. S2A). Larvae with *cry39-Gal4*, *Pdf-Gal80* and *UAS-dTrpA1* transgenes are labeled in Fig. 2C as *DN1 > TrpA1* for simplicity.

Larvae were entrained in LD cycles at 22°C and then shifted to 30°C for 4hr from ZT8 to ZT12 to activate dTrpA1 in DN1s. The enhancer in the *Hr38-Tomato* construct also gives expression in DN1s, allowing us to validate that dTrpA1 induced firing in DN1s. The data in Fig. 2C show that *Hr38-Tomato* levels at ZT12 were 3.2-fold higher in *dTrpA1*-expressing DN1s than in control DN1s that went through the same temperature shift but lacked a *dTrpA1* transgene.

Next we measured *Hr38-Tomato* in LN_vs. The data in Fig. 2C show that *Hr38-Tomato* levels were 1.4-fold lower in LN_vs in larvae in which DN1s were induced to fire than in LN_vs from control larvae (Fig. 2C). Thus increased neuronal activity in DN1s induced *Hr38* expression in DN1s and repressed *Hr38* in LN_vs, which is consistent with DN1s inhibiting LN_v activity.

Next we measured *Pura-Tomato* levels in LN_vs when DN1s were induced to fire from ZT8 to ZT12. The data in Fig. 2C show that *Pura-Tomato* levels in LN_vs at ZT12 were 2.5-fold higher in larvae with dTrpA1 active in DN1s than in control larvae without a *dTrpA1* transgene. Thus inhibiting LN_v activity by activating DN1s increases *Pura* transcription in LN_vs. These data support the conclusion that *Pura* transcription can be activated by transient hyperpolarization.

Expression of *Hr38* and *Pura* is mutually exclusive

The opposite responses of *Hr38* and *Pura* transcription to neuronal activity and hyperpolarization suggest that they are components of mutually exclusive gene expression programs. To test this idea, we simultaneously measured *Hr38* and *Pura* transcription in a single cell. We converted *Hr38-Tomato* to *Hr38-GFP* by replacing tdTomato with GFP but retaining the PEST, NLS and other sequences shown in Fig. 1A. *Hr38-GFP* was inserted to chromosome 3 to generate animals with both *Hr38-GFP* and *Pura-Tomato* transgenes. The data in Fig. S2B show that *Hr38-GFP* levels peaked at ZT2 in LN_vs and had similarly timed rhythms as *Hr38-Tomato*. Thus the temporal pattern of the two *Hr38* reporter genes is independent of the fluorescent protein used and of the genomic insertion site.

Next we measured the levels of *Hr38-GFP* and *Pura-Tomato* in LN_vs at different times of day (Fig. 2D and Fig. S2C). The data show that an individual LN_v has one of three patterns of gene expression: (i) high *Pura-Tomato* and low *Hr38-GFP* levels – most cells at ZT18 (blue dots); (ii) low levels of both reporter genes – most cells at ZT0 (black dots); or (iii) high *Hr38-GFP* and low *Pura-Tomato* levels – many cells at ZT2 (orange dots in graph on right). LN_vs at ZT12 have low Tomato expression and either intermediate or low levels of GFP (Fig. S2D) but were excluded from the graph in Fig. 2D for visual simplicity. The inability to detect LN_vs with high levels of both reporter genes supports the idea that *Hr38* and *Pura* are parts of mutually exclusive transcriptional programs.

Given that *Hr38* and *Pura* transcription is activated by activity and hyperpolarization respectively (Fig. 1C, Fig. 2A-C), it seems likely that the three patterns of reporter expression in LNvs represent three different states of LN_v excitability: hyperpolarized (ZT18), intermediate or resting (ZT0) and excited (ZT2).

Increases in neuronal activity have been measured via immediate early genes such as *c-fos* and also by Calcium sensors such as GCaMP (Morgan et al., 1987; Wang et al., 2003). However, it has been more challenging to detect hyperpolarization or decreases in neuronal activity. The data presented here suggest that transcriptional reporter genes will help distinguish between neurons at rest with low activity and hyperpolarized neurons. In addition, the *Pura* reporter gene could be useful to identify neurons undergoing structural plasticity.

_Hr38_ and _Pura_ respond in opposite directions to activity-dependent transcription factors Creb and Mef2

Mammalian transcription factors such as CREB and Mef2 are post-translationally modified by neuronal firing to activate transcription (Lyons and West, 2011; West and Greenberg, 2011). Indeed, both CREB and Mef2 regulate *Nr4a1*, the mammalian *Hr38* orthologue, in neurons (Fass et al., 2003; Lam et al., 2010). We found three TGACGTCA CREB response elements (CRE) and two AT-enriched Mef2 binding sites clustered within 780bp of the 4kb *Hr38* enhancer that we used to construct the *Hr38-Tomato* reporter gene. Thus CREB and Mef2 were candidates to link neuronal activity to *Hr38* transcription.

To test if CREB can regulate *Hr38* expression, we used a CrebB repressor isoform [*UAS-CrebB repressor* (Yin et al., 1994)] since there are concerns with the available *UAS-CrebB* activator transgenes (Perazzona et al., 2004). We assayed *Hr38-Tomato* levels in LN_vs across the day and found that constitutive expression of CrebB repressor with *Pdf-Gal4* reduced the peak of *Hr38-Tomato* at ZT2 by 2-fold, although there was no statistical difference from control LN_vs at other times (Fig. 3A). A synthetic reporter gene with 4 copies of a CRE gave a similar temporal pattern to *Hr38-Tomato* in LN_vs (Fig. S3A-B) and its expression was also reduced by expressing *CrebB repressor* in LN_vs with *Pdf-Gal4* (Fig. S3B). To test if Mef2 regulates *Hr38* transcription, we used *Pdf-Gal4* to overexpress *Mef2* in LN_vs. The data in Fig. 3A show that *Hr38-Tomato* levels were 1.5-fold higher in Mef2-overexpressing LN_vs than in control LN_vs at ZT0, but not significantly different at other times. Thus Mef2 and Creb contribute to the normal profile of *Hr38* expression, but there must be additional factors involved.

Performing the same experiments with *Pura-Tomato*, we found that *Pura-Tomato* levels in LN_vs were slightly higher in *CrebB* repressor-expressing LN_vs than GFP-expressing controls at ZT12, but not different from control LN_vs at other times (Fig. 3B). However, *Pura-Tomato* levels were at least 2-fold lower in Mef2-overexpressing LN_vs than in control LN_vs at all times of day (Fig. 3B). Repression of *Pura* by Mef2 is consistent with (Sivachenko et al., 2013) who showed that over-expressing Mef2 blocked retraction of s-LN_v projections and left them in a constitutively expanded state. The novel responses of *Pura* to neuronal activity (Fig. 1 & 2) and to Mef2 (Fig. 3B) led us to study *Pura* regulation in more detail.

Dissecting the *Pura* enhancer to identify cis-regulatory elements

We first sought to find the minimal *Pura* enhancer that responds to changes in neuronal activity in LN_vs in order to identify cis-regulatory elements. The 1.5kb *Pura-B* enhancer in Fig. 1B contains the likely transcription start site for *Pura* transcript B and our deletion constructs all used 100bp surrounding this transcription start site as a basal promoter with varying lengths of upstream DNA. The different constructs were inserted into the same chromosomal location as *Pura-Tomato B* and assayed in larval LN_vs.

To identify the minimal *Pura* enhancer that retains the spatial and temporal expression pattern of the full-length enhancer in LN_vs, larvae were entrained in LD and *Pura-Tomato* levels measured at ZT18, the time of peak expression (Fig. 1B). Fig. 4A and Fig. S4A show a series of deletions of the *Pura* enhancer with purple or blue indicating expression or lack of detectable expression in LN_vs, respectively. The smallest transgene that expressed in LN_vs was *Pura-Tomato P*, with only 116bp upstream of regulatory DNA upstream of the basal promoter. Furthermore, *Pura-Tomato P* has the same temporal pattern in LN_vs as *Pura-Tomato A* (Fig. 4B, Fig. S4B).

We then tested if *Pura-Tomato P* responds to neuronal activity and hyperpolarization like the larger constructs. We used *Pdf-Gal4* to express either *UAS-NCB*, *UAS-Kir2.1* or *UAS-GFP* and measured *Pura-Tomato A* and *Pura-Tomato P* levels in LN_vs at ZT12. The data in Fig. 4C show that *Pura-Tomato P* was induced by Kir2.1 and repressed by NCB just like *Pura-Tomato A*. Thus we focused on *Pura-Tomato P* to identify cis-regulatory elements that respond to neuronal activity.

***Pura* is repressed by activity-regulated transcription factors**

The 116bp *Pura* enhancer is highly conserved across 23 *Drosophila* species (Siepel et al., 2005), although this is partly because this region overlaps with a protein coding exon from *Pura* RNA isoforms A and D (Fig. 4A). To predict cis-regulatory elements in the *Pura* enhancer *P*, we used MATCH analysis from TRANSFAC (Kel et al., 2003) and focused on transcription factors known to be regulated by neuronal activity. Our analysis identified one potential Mef2 binding site, two potential Egr-1 binding sites and three potential Atf3 binding sites in *Pura P* (Fig. 4D). These sites are conserved in *D. pseudoobscura* and *D. virilis* (Fig. S4C).

While Mef2 is post-translationally modified by neuronal activity (Flavell et al., 2006), expression of *Egr-1* and *Atf3* are rapidly induced by neuronal activity in mammals (Milbrandt, 1987; Zhang et al., 2011). Expression of the fly *Egr-1* homolog – *stripe* (*sr*) – is rapidly induced by neuronal activity in LN_vs (Chen et al., 2016) and *sr* mRNA is 3.6-fold higher at CT3, when LN_vs are more excitable, than at CT15 (Mizrak et al., 2012). Similarly, *Atf3* mRNA levels in LN_vs are 3.1-fold higher at CT3 than CT15 (Mizrak et al., 2012).

We performed gain- and loss-of-function experiments to test if these transcription factors regulate the minimal *Pura* enhancer. We used *Pdf-Gal4* to target either overexpression or RNAi transgenes to LN_vs and measured *Pura-Tomato P* levels at ZT12. The data in Fig. 4E show that *Pura-Tomato P* levels in LN_vs were reduced by over-expressing Mef2, Sr or Atf3. Over-expressing Atf3 gave the strongest repression, which is consistent with the number of potential Atf3 binding sites (Fig. 4D). We also found that *Pura-Tomato P* levels increased when RNAi targeting any one of these transcription factors was expressed in LN_vs (Fig. 4E). Thus we conclude that Mef2, Sr and Atf3 all repress *Pura* transcription and their effects are likely direct given the predicted binding sites in the minimal *Pura* enhancer.

Mammalian Mef2 is post-translationally modified to rapidly regulate gene expression in response to increased neuronal activity (Flavell et al., 2006). If the same is true in LN_vs, neuronal activity could rapidly activate fly Mef2 to repress transcription of *Pura* and co-regulated genes. With a short delay, the induction of activity-regulated genes such as Sr would cement *Pura* repression for longer – with the duration of repression presumably

depending on the intensity of neuronal activity, the resulting levels of the activity-induced repressors and their intrinsic half-lives.

An E-box in the *Pura* enhancer is not essential for transcriptional activation by hyperpolarization

One sequence that stood out as a potential binding site for a transcriptional activator in the minimal *Pura* enhancer was a CACGTG E-box. This sequence can be directly bound by a dimer of Clock (Clk) and Cycle (Cyc), two core clock components that are bHLH transcription factors. Clk and Cyc drive circadian rhythms in the expression of many genes by interacting with the rhythmically produced repressor protein Period that regulates Clk/Cyc DNA-binding (reviewed by (Hardin, 2011).

To test the importance of this E-box in the response to hyperpolarization, we mutated its core to CA**GC**TG as in (Darlington et al., 1998) and called this reporter gene *Pura-Tomato P mE* for **m**utant E-box. The data in Fig. 4F show that *Pura-Tomato P mE* levels were 10-fold lower than *Pura-Tomato P* levels in LN_vs at ZT12. To test whether the E-box is necessary for the response to hyperpolarization, we used *Pdf-Gal4* to constitutively express *Kir2.1* and compared levels of *Pura-Tomato P mE* at ZT12 with control LN_vs expressing a GFP transgene. We found that levels of *Pura-Tomato P mE* were 3.5-fold higher in *Kir2.1*-expressing LN_vs than in control LN_vs (Fig. 4G). Thus the E-box in the minimal *Pura* enhancer affects *Pura* expression but is not necessary for transcriptional activation by hyperpolarization. We did not test if increased neuronal activity represses *Pura-Tomato P mE* because expression of this reporter gene was too low in control LN_vs to reliably measure potential decreases.

***Pura* is activated by the transcription factor Toy**

As a complementary approach to identifying transcription factors regulating *Pura*, we performed an RNAi screen in LN_vs. We focused on a set of 110 transcription factors we identified that are expressed in fly heads (Adryan and Teichmann, 2006; Celniker et al., 2009; Hughes et al., 2012) and for which there were available short hairpin RNA (shRNA) lines in a common genetic background (Ni et al., 2011). We used *Pdf-Gal4* to express an *shRNA* transgene against each transcription factor and measured *Pura-Tomato B* reporter levels in LN_vs at its peak of ZT18. Only three lines changed *Pura-Tomato B* levels by more than two standard deviations from the mean of control LN_vs

(Fig. 5A, Table S1). Two of these lines increased *Pura-Tomato B* levels by 1.7-fold – these targeted *trachealess* and *pointed*. The third line reduced *Pura-Tomato B* and it stood out since it affected reporter gene levels so dramatically: shRNA targeting *twin-of-eyeless* (*toy*) reduced Tomato levels 5.5-fold compared to control LN_vs, with the next strongest reduction of *Pura-Tomato B* only 1.4-fold (Fig. 5A).

toy encodes one of the two *Drosophila* Pax-6 transcription factors. These proteins have two separate DNA binding domains: a Paired domain and a Homeodomain (Treisman et al., 1991). *toy* is best known as a master regulator of eye development (Czerny et al., 1999) and is also involved in mushroom body development (Kurusu et al., 2000). However, *toy* is also expressed in various neurons in adult flies, including LN_vs (Glossop et al., 2014) and mushroom body neurons (Henry et al., 2012), both of which are sites of structural plasticity (Fernandez et al., 2008; Heisenberg et al., 1995).

To test if Toy regulates the minimal 116bp *Pura* enhancer, we used *Pdf-Gal4* to express *UAS-toy* (Czerny et al., 1999) for overexpression or *UAS-toy-shRNA* or *UAS-toy-RNAi* transgenes to reduce expression. *toy-shRNA* and *toy-RNAi* target different regions of *toy*. The results in Fig. 5B show that *Pura-Tomato P* levels at ZT12 in LN_vs were 2.8-fold higher in *toy*-overexpressing LN_vs and 4- or 5-fold lower with *toy-shRNA* and *toy-RNAi*. Thus we conclude that Toy regulates *Pura*.

We searched for Pax-6 binding sites in the minimal *Pura* enhancer and found one Pax-6 binding site that overlaps with two of the Egr-1 sites and the Mef2 site (Fig. 4D). To test its function, we mutated this Pax-6 site in the context of *Pura-Tomato P* – see STAR methods for details. This mutation also affects the predicted Egr-1 and Mef2 binding sites. Levels of the resulting construct (*Pura-Tomato P mT*) were almost undetectable in LN_vs even at the normal peak of *Pura* expression at ZT18 (Fig. 5C). Thus this Pax-6 site is required for *Pura* expression and leads us to propose that Toy directly regulates *Pura* expression. *Pura-Tomato P mT* could not be activated with *Pdf-Gal4* expressing *UAS-Kir2.1* in LN_vs (Fig. S5). However, the very low levels of *Pura-Tomato P mT* expression mean that we cannot make a strong conclusion that this Pax-6 site is required for induction by hyperpolarization.

***toy* transcription is activated by hyperpolarization**

Since the repressors that regulate *Pura* expression are likely regulated by post-translational modification (Mef2) or by gene expression (Sr, Atf3), we wanted to test if *toy* also responds to neuronal activity. We first measured Toy protein levels in LN_vs at different times of day and found that Toy levels change over 24hr in LN_vs (Fig. 5D). Toy protein levels peak at ZT18, in phase with *Pura* transcription (Fig. 1B). Next we tested if Toy levels are regulated by neuronal activity. We measured Toy protein levels at ZT12 in LN_vs with *Pdf-Gal4* expressing *Kir2.1*, *NCB* or GFP as a control. The data in Fig. 5E show that Toy levels were 1.5-fold higher in *Kir2.1*-expressing LN_vs and 1.2-fold lower in *NCB*-expressing LN_vs than control LN_vs. Thus Toy protein levels are slightly altered by neuronal activity.

To test if *toy* is also transcriptionally regulated in LN_vs, we sought to find the relevant enhancer for LN_v expression. Two overlapping *toy* enhancers (R9G08 and R9G09) appear to drive expression in LN_vs (Jenett et al., 2012). This 1.1kb overlapping region is highly conserved across 23 *Drosophila* species. We generated a *toy* transcriptional reporter by fusing the *toy* enhancer R9G08 plus 87bp from R9G09 to an *Hsp70* basal promoter and destabilized tdTomato. The data in Fig. 5F show that *toy-Tomato* levels change over 24hr in LN_vs. *toy-Tomato* levels increased 2.5-fold between ZT12 and ZT18, when LN_vs become more hyperpolarized (Cao and Nitabach, 2008).

We hypothesized that the increase of *toy-Tomato* from ZT12 to ZT18 is driven by hyperpolarization. To test this idea, we measured *toy-Tomato* levels at ZT12 in LN_vs expressing Kir2.1. The data in Fig. 5G show that *toy-Tomato* levels were 5.8-fold higher in *Kir2.1*-expressing LN_vs than in control LN_vs. However, there was no difference in *toy-Tomato* levels between *NCB*-expressing and control LN_vs at ZT12. Thus we conclude that *toy* transcription is induced by hyperpolarization.

Thus we propose that hyperpolarization induces *toy* transcription and the resulting Toy protein then activates *Pura*. This indirect activation of *Pura* by hyperpolarization presumably adds a time delay between hyperpolarization and *Pura* transcription. We speculate that this delay is important and only allows *Pura* expression in response to prolonged hyperpolarization. If a neuron started firing again after a relatively short period of hyperpolarization, then this would induce activity-dependent transcription repressors

such as Sr and Mef2, which likely compete with Toy for binding to the *Pura* enhancer since the binding sites for Sr and Mef2 overlap the Toy binding site (Fig. 4D). Thus we propose that this mechanism allows the *Pura* enhancer to report the recent electrical history of an individual LN_v – as seen in Fig. 2D.

Discussion

Transcription of genes such as *c-fos* is rapidly induced in mammalian neurons in response to increased neuronal activity. Many of these immediate early genes encode transcription factors that regulate a second set of genes and overall these two waves of gene expression stabilize changes in the excitability and connectivity of neurons in response to firing (West and Greenberg, 2011). Here we describe a complementary gene expression program that is activated in response to hyperpolarization or neuronal inactivity. Using *Drosophila* LN_vs as model neurons, we showed that transcription of the gene encoding the Pax-6 transcription factor Toy is induced by hyperpolarization. Toy then activates transcription of *Pura*, a "plasticity gene" which encodes a Rho1 GEF that increases Rho1 activity and helps retract s-LN_v projections to reduce their signaling potency (Fig. 6) (Petsakou et al., 2015). Although many of our experiments used the mammalian Kir2.1 channel to induce hyperpolarization, the *Pura* transcriptional reporter normally shows a 24hr rhythm in LN_vs and can also be induced via an inhibitory neural circuit.

If one function of the gene expression program induced by neuronal inactivity is to retract projections, then it makes sense that the activity-induced gene expression program would need to block a pre-existing program with an opposite effect on plasticity. Indeed, the rapid induction of repressors such as Egr-1 / Sr in response to neuronal activity in both mammals and flies (Milbrandt, 1987; Chen et al., 2016) suggests that repressing an alternative gene expression program is a conserved feature of how neurons respond to firing. Data supporting this idea comes from studying genes whose expression is altered by singing in the zebra finch brain: singing induced the expression of hundreds of genes and simultaneously repressed hundreds of different genes (Whitney et al., 2014). It would be interesting to know if the genes repressed by singing are induced by hyperpolarization or neuronal inactivity. Intriguingly, blocking neuronal activity in cultured mouse cortical neurons induced the expression of many genes (Schaukowitch et al., 2017), suggesting that a gene expression program that responds to neuronal inactivity exists in mammals.

We found that an individual LN_v shifts from expressing high levels of *Pura-Tomato* to expressing *Hr38-GFP* and repressing *Pura-Tomato* within 8 hours and we did not find any LN_vs that expressed high levels of both *Hr38-GFP* and *Pura-Tomato*. Thus the

activity- and inactivity-regulated gene expression programs are coordinated to be mutually exclusive, which fits with their likely biological functions. Mechanistically, the minimal *Pura* enhancer has overlapping binding sites for Sr and Toy. This offers a potential mechanism for how the *Pura* enhancer can integrate the recent activity of LN_vs and decide whether or not to activate *Pura* transcription.

There are many genes whose transcription increases in response to firing. So far, we only know of 2 genes – *toy* and *Pura* – whose transcription is induced by hyperpolarization. While it is probably premature to call this a gene expression program, the induction of the transcription factor Toy as a putative first responder makes it likely that it will have multiple target genes. Furthermore, we previously identified many genes whose expression was activated by hyperpolarizing LN_vs (Mizrak et al., 2012). However, we do not yet know if these genes are regulated transcriptionally and whether they are targets of Toy.

It will be interesting to know if inactivity-driven gene expression is a general property of neurons. Intriguingly, *toy* expression persists in adult mushroom body neurons, indicative of a function in mature neurons and Pax6 is present in cortical neurons, a major site of plasticity in the mammalian brain (Zhang et al., 2014).

The intracellular signaling pathways that are activated by neuronal firing and lead to induction of gene expression are well-understood: increases in Ca^{2+} and cyclic AMP activate kinase and phosphatase pathways that post-translationally activate pre-existing transcription factors such as Creb and Mef2 (Flavell et al., 2006; Gonzalez et al., 1989). However, we do not yet know how *toy* transcription is activated in response to neuronal inactivity or hyperpolarization. One possibility is that a novel signaling pathway is activated by hyperpolarization. However, we consider it more likely that low levels of a second messenger such as Ca^{2+} and cyclic AMP activate *toy* transcription. This idea is appealing for two reasons. First, it fits with the observation of mutually exclusive *Pura* and *Hr38* gene expression: if the same signaling molecule triggers both gene expression programs but at very different concentrations, then the two programs would be coordinated since it would be impossible for the signal to simultaneously be at both high and low concentrations. Second, it seems likely to take longer for a signal to decay back to basal levels than for a signal to arise in the first place. While it may be advantageous

for a neuron to rapidly respond to firing to strengthen synapses, we believe that a neuron should only start to induce a synaptic retraction or pruning program with slow kinetics.

One situation in which there may be prolonged low levels of neuronal activity in the brain is sleep. Synaptic downscaling has been reported to reduce the overall connectivity of the brain (de Vivo et al., 2017; Diering et al., 2017). We speculate that a gene expression program activated by neuronal inactivity could sweep through parts of the brain during sleep and restore the brain to a similar level of connectivity as on waking the previous day. However, strong memories would persist either due to the intensity of firing in these neurons the previous day that makes it harder to remove the activity-dependent program during sleep or perhaps even because those memories are replayed during sleep – and therefore the neurons reactivated – as seen in rats after learning a spatial navigation task (Lee and Wilson, 2002). This could even explain why sensory inputs are damped during sleep and why sleep typically lasts for so many hours.

Acknowledgements

We are indebted to numerous stock centers for sharing flies, antibodies and plasmids: the HHMI Janelia Farm Research Campus, the Vienna Drosophila Resource Center (VDRC), the Bloomington *Drosophila* Stock Center (supported by NIH P40OD018537), the Developmental Studies Hybridoma Bank (created by the NICHD and maintained at The University of Iowa), the TRiP stock center at Harvard Medical School (supported by NIGMS, NIH) and FlyORF (Bischof et al., 2013). We thank Claude Desplan for Toy antibodies, Gerry Rubin's lab for plasmids, Jia Ling for advice on basal promoters, Jens Rister for advice on generating mutants, Matthieu Cavey for advice on confocal microscopy and Chris Hackley for advice on cloning. We thank Esteban Mazzoni, Tom Carew, Adam Carter, Claude Desplan, Erich Jarvis and Niels Ringstad for advice and support and Claude Desplan, Simon Kidd, Alison Ehrlich and Kyla Hamling for comments on the manuscript. We are indebted to Dogukan Mizrak and Marc Ruben for deciding to profile LN_vs in altered electrical states and to Subhabrata Sanyal for sharing his activity reporter genes. This investigation was conducted in facilities constructed with support from Research Facilities Improvement Grant Number C06 RR-15518-01 from the NIH National Center for Research Resources. Imaging was performed at the NYU Center for Genomics & Systems Biology. ZZ was partly supported by the MacCracken Program and a James Arthur Dissertation Fellowship from NYU's Graduate School of Arts and Science. Work in the authors' laboratories is supported by BSF grant 2015506 (SK and JB) and NIH grant GM063911 (JB).

Author contribution

ZZ and JB conceived and designed the study. ZZ performed all experiments and data analysis except that TSO stained Toy in wild type LN_vs. SM and SK provided the codon-optimized tdTomato plasmid prior to publication. ZZ and JB interpreted the results and wrote the manuscript. JB supervised the project and provided funding.

References

Adryan, B., and Teichmann, S.A. (2006). FlyTF: a systematic review of site-specific transcription factors in the fruit fly *Drosophila melanogaster*. Bioinformatics *22*, 1532-1533.

Baines, R.A., Uhler, J.P., Thompson, A., Sweeney, S.T., and Bate, M. (2001). Altered electrical properties in *Drosophila* neurons developing without synaptic transmission. J. Neuroscience *21*, 1523-1531.

Bischof, J., Bjorklund, M., Furger, E., Schertel, C., Taipale, J., and Basler, K. (2013). A versatile platform for creating a comprehensive UAS-ORFeome library in *Drosophila*. Development *140*, 2434-2442.

Cao, G., and Nitabach, M.N. (2008). Circadian control of membrane excitability in *Drosophila melanogaster* lateral ventral clock neurons. J. Neuroscience *28*, 6493-6501.

Celniker, S.E., Dillon, L.A., Gerstein, M.B., Gunsalus, K.C., Henikoff, S., Karpen, G.H., Kellis, M., Lai, E.C., Lieb, J.D., MacAlpine, D.M.*, et al.* (2009). Unlocking the secrets of the genome. Nature *459*, 927-930.

Chen, X., Rahman, R., Guo, F., and Rosbash, M. (2016). Genome-wide identification of neuronal activity-regulated genes in *Drosophila*. eLife *5*, e19942.

Collins, B., Kane, E.A., Reeves, D.C., Akabas, M.H., and Blau, J. (2012). Balance of activity between LN_vs and glutamatergic dorsal clock neurons promotes robust circadian rhythms in *Drosophila*. Neuron *74*, 706-718.

Czerny, T., Halder, G., Kloter, U., Souabni, A., Gehring, W.J., and Busslinger, M. (1999). t*win of eyeless*, a second *Pax6* gene of *Drosophila*, acts upstream of *eyeless* in the control of eye development. Molecular Cell *3*, 297-307.

Darlington, T.K., Wager-Smith, K., Ceriani, M.F., Staknis, D., Gekakis, N., Steeves, T.D., Weitz, C.J., Takahashi, J.S., and Kay, S.A. (1998). Closing the circadian loop: CLOCK-induced transcription of its own inhibitors *per* and *tim*. Science *280*, 1599-1603.

de Vivo, L., Bellesi, M., Marshall, W., Bushong, E.A., Ellisman, M.H., Tononi, G., and Cirelli, C. (2017). Ultrastructural evidence for synaptic scaling across the wake/sleep cycle. Science *355*, 507-510.

Diering, G.H., Nirujogi, R.S., Roth, R.H., Worley, P.F., Pandey, A., and Huganir, R.L. (2017). Homer1a drives homeostatic scaling-down of excitatory synapses during sleep. Science *355*, 511-515.

Ebert, D.H., and Greenberg, M.E. (2013). Activity-dependent neuronal signalling and autism spectrum disorder. Nature *493*, 327-337.

Fass, D.M., Butler, J.E., and Goodman, R.H. (2003). Deacetylase activity is required for cAMP activation of a subset of CREB target genes. J. Biol Chem *278*, 43014-43019.
Fernandez, M.P., Berni, J., and Ceriani, M.F. (2008). Circadian remodeling of neuronal circuits involved in rhythmic behavior. PLoS Biology *6*, e69.
Flavell, S.W., Cowan, C.W., Kim, T.K., Greer, P.L., Lin, Y., Paradis, S., Griffith, E.C., Hu, L.S., Chen, C., and Greenberg, M.E. (2006). Activity-dependent regulation of MEF2 transcription factors suppresses excitatory synapse number. Science *311*, 1008-1012.
Fujita, N., Nagata, Y., Nishiuchi, T., Sato, M., Iwami, M., and Kiya, T. (2013). Visualization of neural activity in insect brains using a conserved immediate early gene, *Hr38*. Current Biology *23*, 2063-2070.
Glausier, J.R., and Lewis, D.A. (2013). Dendritic spine pathology in schizophrenia. Neuroscience *251*, 90-107.
Glossop, N.R., Gummadova, J.O., Ghangrekar, I., Hardin, P.E., and Coutts, G.A. (2014). Effects of TWIN-OF-EYELESS on clock gene expression and central-pacemaker neuron development in *Drosophila*. J. Biol Rhythms *29*, 151-166.
Gonzalez, G.A., Yamamoto, K.K., Fischer, W.H., Karr, D., Menzel, P., Biggs, W., 3rd, Vale, W.W., and Montminy, M.R. (1989). A cluster of phosphorylation sites on the cyclic AMP-regulated nuclear factor CREB predicted by its sequence. Nature *337*, 749-752.
Groth, A.C., Fish, M., Nusse, R., and Calos, M.P. (2004). Construction of transgenic *Drosophila* by using the site-specific integrase from phage phiC31. Genetics *166*, 1775-1782.
Hamada, F.N., Rosenzweig, M., Kang, K., Pulver, S.R., Ghezzi, A., Jegla, T.J., and Garrity, P.A. (2008). An internal thermal sensor controlling temperature preference in *Drosophila*. Nature *454*, 217-220.
Hardin, P.E. (2011). Molecular genetic analysis of circadian timekeeping in *Drosophila*. Advances in Genetics *74*, 141-173.
Heisenberg, M. (2003). Mushroom body memoir: from maps to models. Nature Reviews Neuroscience *4*, 266-275.
Heisenberg, M., Heusipp, M., and Wanke, C. (1995). Structural plasticity in the *Drosophila* brain. J. Neuroscience *15*, 1951-1960.
Henry, G.L., Davis, F.P., Picard, S., and Eddy, S.R. (2012). Cell type-specific genomics of *Drosophila* neurons. Nucleic Acids Research *40*, 9691-9704.

Hughes, M.E., Grant, G.R., Paquin, C., Qian, J., and Nitabach, M.N. (2012). Deep sequencing the circadian and diurnal transcriptome of *Drosophila* brain. Genome Research *22*, 1266-1281.

Jenett, A., Rubin, G.M., Ngo, T.T., Shepherd, D., Murphy, C., Dionne, H., Pfeiffer, B.D., Cavallaro, A., Hall, D., Jeter, J.*, et al.* (2012). A GAL4-driver line resource for *Drosophila* neurobiology. Cell Reports *2*, 991-1001.

Kandel, E.R., Dudai, Y., and Mayford, M.R. (2014). The molecular and systems biology of memory. Cell *157*, 163-186.

Kel, A.E., Gossling, E., Reuter, I., Cheremushkin, E., Kel-Margoulis, O.V., and Wingender, E. (2003). MATCH: A tool for searching transcription factor binding sites in DNA sequences. Nucleic Acids Research *31*, 3576-3579.

Kurusu, M., Nagao, T., Walldorf, U., Flister, S., Gehring, W.J., and Furukubo-Tokunaga, K. (2000). Genetic control of development of the mushroom bodies, the associative learning centers in the *Drosophila* brain, by the *eyeless*, *twin of eyeless*, and *Dachshund* genes. PNAS *97*, 2140-2144.

Kvon, E.Z., Kazmar, T., Stampfel, G., Yanez-Cuna, J.O., Pagani, M., Schernhuber, K., Dickson, B.J., and Stark, A. (2014). Genome-scale functional characterization of *Drosophila* developmental enhancers in vivo. Nature *512*, 91-95.

Lam, B.Y., Zhang, W., Ng, D.C., Maruthappu, M., Roderick, H.L., and Chawla, S. (2010). CREB-dependent *Nur77* induction following depolarization in PC12 cells and neurons is modulated by MEF2 transcription factors. J. Neurochem *112*, 1065-1073.

Lee, A.K., and Wilson, M.A. (2002). Memory of sequential experience in the hippocampus during slow wave sleep. Neuron *36*, 1183-1194.

Lee, T., and Luo, L. (1999). Mosaic analysis with a repressible cell marker for studies of gene function in neuronal morphogenesis. Neuron *22*, 451-461.

Leslie, J.H., and Nedivi, E. (2011). Activity-regulated genes as mediators of neural circuit plasticity. Progress in Neurobiology *94*, 223-237.

Lyons, M.R., and West, A.E. (2011). Mechanisms of specificity in neuronal activity-regulated gene transcription. Progress in Neurobiology *94*, 259-295.

Mao, Z., Bonni, A., Xia, F., Nadal-Vicens, M., and Greenberg, M.E. (1999). Neuronal activity-dependent cell survival mediated by transcription factor MEF2. Science *286*, 785-790.

Martin, J.R., Ernst, R., and Heisenberg, M. (1998). Mushroom bodies suppress locomotor activity in *Drosophila melanogaster*. Learning & Memory *5*, 179-191.

Mathelier, A., Fornes, O., Arenillas, D.J., Chen, C.Y., Denay, G., Lee, J., Shi, W., Shyr, C., Tan, G., Worsley-Hunt, R.*, et al.* (2016). JASPAR 2016: a major expansion and update of the open-access database of transcription factor binding profiles. Nucleic Acids Research *44*, D110-115.
McGuire, S.E., Le, P.T., Osborn, A.J., Matsumoto, K., and Davis, R.L. (2003). Spatiotemporal rescue of memory dysfunction in *Drosophila*. Science *302*, 1765-1768.
Mezan, S., Feuz, J.D., Deplancke, B., and Kadener, S. (2016). PDF signaling is an integral part of the *Drosophila* circadian molecular oscillator. Cell Reports *17*, 708-719.
Milbrandt, J. (1987). A nerve growth factor-induced gene encodes a possible transcriptional regulatory factor. Science *238*, 797-799.
Milbrandt, J. (1988). Nerve growth factor induces a gene homologous to the glucocorticoid receptor gene. Neuron *1*, 183-188.
Mizrak, D., Ruben, M., Myers, G.N., Rhrissorrakrai, K., Gunsalus, K.C., and Blau, J. (2012). Electrical activity can impose time of day on the circadian transcriptome of pacemaker neurons. Current Biology *22*, 1871-1880.
Morgan, J.I., Cohen, D.R., Hempstead, J.L., and Curran, T. (1987). Mapping patterns of *c-fos* expression in the central nervous system after seizure. Science *237*, 192-197.
Murphy, T.H., and Corbett, D. (2009). Plasticity during stroke recovery: from synapse to behaviour. Nature Reviews Neuroscience *10*, 861-872.
Ni, J.Q., Zhou, R., Czech, B., Liu, L.P., Holderbaum, L., Yang-Zhou, D., Shim, H.S., Tao, R., Handler, D., Karpowicz, P.*, et al.* (2011). A genome-scale shRNA resource for transgenic RNAi in *Drosophila*. Nature Methods *8*, 405-407.
Nitabach, M.N., Wu, Y., Sheeba, V., Lemon, W.C., Strumbos, J., Zelensky, P.K., White, B.H., and Holmes, T.C. (2006). Electrical hyperexcitation of lateral ventral pacemaker neurons desynchronizes downstream circadian oscillators in the fly circadian circuit and induces multiple behavioral periods. J. Neuroscience *26*, 479-489.
Park, J.H., Helfrich-Forster, C., Lee, G., Liu, L., Rosbash, M., and Hall, J.C. (2000). Differential regulation of circadian pacemaker output by separate clock genes in *Drosophila*. PNAS *97*, 3608-3613.
Perazzona, B., Isabel, G., Preat, T., and Davis, R.L. (2004). The role of cAMP response element-binding protein in *Drosophila* long-term memory. J. Neuroscience *24*, 8823-8828.
Petsakou, A., Sapsis, T.P., and Blau, J. (2015). Circadian rhythms in Rho1 activity regulate neuronal plasticity and network hierarchy. Cell *162*, 823-835.

Pfeiffer, B.D., Jenett, A., Hammonds, A.S., Ngo, T.T., Misra, S., Murphy, C., Scully, A., Carlson, J.W., Wan, K.H., Laverty, T.R.*, et al.* (2008). Tools for neuroanatomy and neurogenetics in *Drosophila*. PNAS *105*, 9715-9720.

Pfeiffer, B.D., Ngo, T.T., Hibbard, K.L., Murphy, C., Jenett, A., Truman, J.W., and Rubin, G.M. (2010). Refinement of tools for targeted gene expression in *Drosophila*. Genetics *186*, 735-755.

Pfeiffer, B.D., Truman, J.W., and Rubin, G.M. (2012). Using translational enhancers to increase transgene expression in *Drosophila*. PNAS *109*, 6626-6631.

Picot, M., Cusumano, P., Klarsfeld, A., Ueda, R., and Rouyer, F. (2007). Light activates output from evening neurons and inhibits output from morning neurons in the *Drosophila* circadian clock. PLoS Biology *5*, e315.

Ruben, M., Drapeau, M.D., Mizrak, D., and Blau, J. (2012). A mechanism for circadian control of pacemaker neuron excitability. J. Biol Rhythms *27*, 353-364.

Schaukowitch, K., Reese, A.L., Kim, S.K., Kilaru, G., Joo, J.Y., Kavalali, E.T., and Kim, T.K. (2017). An intrinsic transcriptional program underlying synaptic scaling during activity suppression. Cell Reports *18*, 1512-1526.

Siepel, A., Bejerano, G., Pedersen, J.S., Hinrichs, A.S., Hou, M., Rosenbloom, K., Clawson, H., Spieth, J., Hillier, L.W., Richards, S.*, et al.* (2005). Evolutionarily conserved elements in vertebrate, insect, worm, and yeast genomes. Genome Research *15*, 1034-1050.

Sivachenko, A., Li, Y., Abruzzi, K.C., and Rosbash, M. (2013). The transcription factor Mef2 links the *Drosophila* core clock to *Fas2*, neuronal morphology, and circadian behavior. Neuron *79*, 281-292.

Stoleru, D., Peng, Y., Agosto, J., and Rosbash, M. (2004). Coupled oscillators control morning and evening locomotor behaviour of *Drosophila*. Nature *431*, 862-868.

Treisman, J., Harris, E., and Desplan, C. (1991). The paired box encodes a second DNA-binding domain in the paired homeo domain protein. Genes & Development *5*, 594-604.

Venken, K.J., He, Y., Hoskins, R.A., and Bellen, H.J. (2006). P[acman]: a BAC transgenic platform for targeted insertion of large DNA fragments in *D. melanogaster*. Science *314*, 1747-1751.

Wang, J.W., Wong, A.M., Flores, J., Vosshall, L.B., and Axel, R. (2003). Two-photon calcium imaging reveals an odor-evoked map of activity in the fly brain. Cell *112*, 271-282.

West, A.E., and Greenberg, M.E. (2011). Neuronal activity-regulated gene transcription in synapse development and cognitive function. Cold Spring Harbor Perspectives in Biology *3*.

Whitney, O., Pfenning, A.R., Howard, J.T., Blatti, C.A., Liu, F., Ward, J.M., Wang, R., Audet, J.N., Kellis, M., Mukherjee, S.*, et al.* (2014). Core and region-enriched networks of behaviorally regulated genes and the singing genome. Science *346*, 1256780.

Yang, Y., Yamada, T., Hill, K.K., Hemberg, M., Reddy, N.C., Cho, H.Y., Guthrie, A.N., Oldenborg, A., Heiney, S.A., Ohmae, S.*, et al.* (2016). Chromatin remodeling inactivates activity genes and regulates neural coding. Science *353*, 300-305.

Yin, J.C., Wallach, J.S., Del Vecchio, M., Wilder, E.L., Zhou, H., Quinn, W.G., and Tully, T. (1994). Induction of a dominant negative CREB transgene specifically blocks long-term memory in *Drosophila*. Cell *79*, 49-58.

Yuan, Q., Xiang, Y., Yan, Z., Han, C., Jan, L.Y., and Jan, Y.N. (2011). Light-induced structural and functional plasticity in *Drosophila* larval visual system. Science *333*, 1458-1462.

Zhang, S.J., Buchthal, B., Lau, D., Hayer, S., Dick, O., Schwaninger, M., Veltkamp, R., Zou, M., Weiss, U., and Bading, H. (2011). A signaling cascade of nuclear calcium-CREB-ATF3 activated by synaptic NMDA receptors defines a gene repression module that protects against extrasynaptic NMDA receptor-induced neuronal cell death and ischemic brain damage. J. Neuroscience *31*, 4978-4990.

Zhang, Y., Chen, K., Sloan, S.A., Bennett, M.L., Scholze, A.R., O'Keeffe, S., Phatnani, H.P., Guarnieri, P., Caneda, C., Ruderisch, N.*, et al.* (2014). An RNA-sequencing transcriptome and splicing database of glia, neurons, and vascular cells of the cerebral cortex. J. Neuroscience *34*, 11929-11947.

Figure Legends

Figure 1. *Hr38* and *Pura* transcription respond in opposite directions to neuronal activity and hyperpolarization.

(A) Schematic of *Hr38* and *Pura* gene loci and reporter genes. Gene structures of *Hr38* and *Pura* are shown with exons as white boxes, introns as thick black lines and intergenic regions as thin black lines. Enhancers tested are shown above the gene models and colored either grey (no expression in larval LN_vs when crossed to GFP) or purple (expression in LN_vs, Fig. S1A). For transcriptional reporter genes, enhancers were fused upstream of a basal promoter (transcription start site denoted by arrow), an intervening sequence (IVS, blue), a synthetic 5'UTR (Syn21, orange), tdTomato cDNA (red), 3 nuclear localization sequences (NLS, green) and a PEST sequence (yellow) to destabilize tdTomato.

(B) *Hr38* and *Pura* transcriptional reporters have differently phased rhythms. Larvae with either *Hr38-* or *Pura-Tomato* transgenes were entrained in LD cycles at 25°C. Third instar larval brains were dissected at the times shown and stained with antibodies to PDF to mark LN_vs (blue) and Tomato (red).

Left: Representative confocal images. The same confocal settings were applied to each scan for all timepoints in one experiment.

Right: Tomato signals in a single LN_v were quantified and normalized to the average value at the peak time for each reporter. Error bars show SEM. The graph is an average of 2 independent experiments with 15-20 single LN_vs from 5 brains in each experiment. The white:black bar on the x-axis represents time in 12:12 LD cycles. The data from ZT0 are replotted at ZT24. Levels of *Hr38-* (black) *and Pura-Tomato* (purple) vary with time in larval LN_vs (one-way ANOVA, $p < 0.0001$).

(C) *Hr38* and *Pura* transcriptional reporter genes respond to long-term hyperexcitation and hyperpolarization in opposite directions. Tomato levels were measured in LN_vs at ZT24 from larvae with either *Hr38-* or *Pura-Tomato* transgenes and *Pdf-Gal4* (*Pdf >*) expressing *UAS-Kir2.1* (*Kir2.1*) for hyperpolarization, *UAS-GFP* (*GFP*) as control or *UAS-NaChBac* (*NCB*) for hyperexcitation. Larval brains were dissected, stained and quantified as in Fig. 1B with representative confocal images on the left and quantification on the right. Tomato signals in single LN_vs were normalized to the average of the control group. *Hr38-Tomato* levels are higher in *NCB*-expressing LN_vs (red) and lower in *Kir2.1*-expressing LN_vs (blue) than *GFP*-expressing LN_vs (Student's *t* test, *NCB* vs *GFP* $p < 0.0001$, *Kir2.1* vs *GFP* $p < 0.001$). *Pura-Tomato* levels are lower in *NCB-*

expressing LN_vs and higher in *Kir2.1*-expressing LN_vs than in *GFP*-expressing LN_vs. (Student's *t*-test, *NCB* vs *GFP* $p < 0.05$, *Kir2.1* vs *GFP* $p < 0.0001$). Error bars show SEM. The graph is an average of 2 independent experiments with 15-20 single cells from 5 brains in each experiment.

Figure 2. *Hr38* and *Pura* transcription respond in opposite directions to transient changes in neuronal activity.

(A) Responses to inducing LN_v firing. Larvae with *Pdf-Gal4* and either *Hr38-* or *Pura-Tomato* were raised at 22°C in LD cycles. Control larvae had no *UAS* transgene (*Pdf* > +, black). Experimental larvae had a *UAS-dTrpA1* transgene (*Pdf* > *dTrpA1*, red). Larvae were shifted to 30°C from ZT12 to ZT16 to activate dTrpA1 and induce LN_v firing – see timeline on bottom right. Larval brains were dissected at ZT16 and stained and quantified as in Fig. 1B. Left: representative confocal images with Tomato (red) and PDF to mark LN_vs (blue) on left and Tomato single channel images on the right. Dashed lines circle LN_v nuclei for quantification. Right: quantification of 2 independent experiments with 15-20 single cells from 5 brains in each experiment. *Hr38-Tomato* levels are higher in *dTrpA1*-expressing LN_vs than in control LN_vs (Student's *t*-test, $p < 0.0001$). *Pura-Tomato* levels are lower in *dTrpA1*-expressing LN_vs than in control LN_vs (Student's *t*-test, $p < 0.0001$). Error bars show SEM.

(B) Responses to inducing LN_v hyperpolarization. Larvae with *Pdf-Gal4*, *tub-Gal80^{ts}* and either *Hr38-* or *Pura-Tomato* were raised at 18°C in LD cycles. Control larvae had no *UAS* transgene (*Pdf, tub-Gal80^{ts}* > +). Experimental larvae had a *UAS-Kir2.1* transgene whose expression was suppressed at 18°C by Gal80 (*Pdf, tub-Gal80^{ts}* > *Kir2.1*). Larvae were shifted to 30°C at ZT22 and maintained in the dark for 4hr before dissection at CT2 – see timeline, bottom right. Staining and quantification were as in Fig. 1B. Left: representative confocal images as in Fig. 2A. Right: quantification of 2 independent experiments with 15-20 single cells from 5 brains in each experiment. *Hr38-Tomato* levels were lower in *Kir2.1*-expressing LN_vs than in control larvae (Student's *t*-test, $p < 0.0001$). *Pura-Tomato* levels were higher in *Kir2.1*-expressing LN_vs than in control LN_vs (Student's *t*-test, $p < 0.0001$). Error bars show SEM.

(C) Responses in LN_vs and DN1s to activating DN1s. Larvae with *cry39-Gal4* and *Pdf-Gal80* expressing UAS transgenes in DN1s (*DN1* >) and *Hr38- or Pura-Tomato* were raised at 22°C in LD cycles. Larvae were shifted to 30°C at ZT8 for 4hr before dissection at ZT12 – see timeline. Larval brains were stained with antibodies to GFP to

mark DN1s (green), PDF to mark LN_vs (blue) and Tomato (red). Quantification as in Fig. 1B with averages from 2 independent experiments containing 10 DN1s or 15-20 LN_vs from 5 brains in each experiment.

Far left: illustration shows that inducing neuronal activity in DN1s (green) inhibits LN_v (blue).

Left: Representative confocal images are shown as in Fig. 2A.

Top left: Control larvae had *UAS-nGFP* (*DN1 > nGFP*) and the experimental group had *UAS-nGFP* and *UAS-dTrpA1* transgenes (*DN1 > nGFP + dTrpA1*). *Hr38-Tomato* levels were higher in *dTrpA1*-expressing DN1s than in control larvae (Student's *t*-test, $p < 0.001$) but lower in LN_vs of larvae in which DN1s were induced to fire (Student's *t*-test, $p < 0.001$). Bottom left: Genotypes as above except that the reporter gene was *Pura-Tomato*. Levels of *Pura-Tomato* were higher in LN_vs of larvae with dTrpA1 activated in DN1s than in control LN_vs (Student's *t*-test, $p < 0.0001$). Error bars show SEM.

(D) *Hr38* and *Pura* reporters give mutually exclusive expression in individual LN_vs.

Larvae with both *Hr38-GFP* and *Pura-Tomato* reporter genes were entrained in LD cycles at 25°C. Third instar larval brains were dissected at the times shown and stained with antibodies to GFP (green), Tomato (red) and PDF to mark LN_vs (blue).

Left: Representative confocal images with time of day indicated above. In single channel images, dashed lines circle the area for quantification.

Top right: GFP and Tomato levels in single LN_vs were quantified, normalized to the maximal levels of all measured time points and plotted against each other. Each dot indicates the measurement of a single LN_v with color indicating measured time: ZT0 – black; ZT2 – orange; ZT18 – blue.

Bottom right: the ratio of GFP to Tomato levels was normalized to the average of the trough time point (ZT18). Error bars show SEM. The graph is an average of 2 independent experiments with 15-20 single cells from 5 brains in each experiment. Data from ZT0 are replotted at ZT24. GFP / Tomato levels vary with time (one-way ANOVA, $p < 0.0001$).

Figure 3. *Hr38* and *Pura* respond in opposite directions to activity-dependent transcription factor Creb and Mef2

Larvae with *Pdf-Gal4* and either *Hr38-* or *Pura-Tomato* transgenes were entrained in LD cycles at 25°C. Larval brains were dissected, stained and quantified as in Fig. 1B. Error bars show SEM. Data from ZT0 is replotted at ZT24. Each dataset is an average of 2

independent experiments with 15-20 single cells from 5 brains in each experiment. In all cases, control larvae had *Pdf-Gal4* expressing a *UAS-GFP* transgene (*Pdf > GFP*).

(A) Responses of *Hr38-Tomato* to Creb and Mef2

Left: Peak *Hr38* expression is reduced by CrebB repressor. Quantification of *Hr38-Tomato* levels in control (*Pdf > GFP*, black) and experimental larvae expressing a *UAS-CrebB repressor* transgene in LN_vs (*Pdf > CrebB repressor*, red). *Hr38-Tomato* levels were lower in *Pdf > CrebB repressor* than in control LN_vs at ZT2 (Student's *t*-test, $p < 0.0001$), but not at other times.

Right: *Hr38* is activated by Mef2 at ZT0. Quantification of *Hr38-Tomato* levels in control (*Pdf > GFP*, black) and experimental larvae expressing a *UAS-Mef2* transgene in LN_vs (*Pdf > Mef2*, red). *Hr38-Tomato* levels were higher in *Pdf > Mef2* LN_vs than in control larvae at ZT0 (Student's *t*-test, $p < 0.01$), but not at other times.

(B) Responses of *Pura-Tomato* to Creb and Mef2

Left: *Pura* is activated by CrebB repressor at ZT12. Quantification of *Pura-Tomato* levels in control (*Pdf > GFP*, black) and experimental larvae expressing a *UAS-CrebB repressor* transgene in LN_vs (*Pdf > CrebB repressor*, red). *Pura-Tomato* levels were higher in *Pdf > CrebB repressor* than in control LN_vs at ZT12 (Student's *t*-test, $p < 0.001$), but not at other times.

Right: *Pura* is repressed by Mef2 at all times. Quantification of *Pura-Tomato* levels in control (*Pdf > GFP*, black) and experimental larvae expressing a *UAS-Mef2* transgene in LN_vs (*Pdf > Mef2*, red). *Pura-Tomato* levels were higher in *Mef2*-expressing than in control larvae at all times tested (Student's *t*-test, $p < 0.0001$ for ZT0, 2 and 18, $p < 0.01$ for ZT6).

Figure 4. The *Pura* enhancer contains cis-regulatory elements for activity-regulated transcription factors.

(A) A minimal *Pura* enhancer for LN_v expression. Map of the *Pura* regulatory region showing exons (grey boxes), introns (black lines) and the transcription start site (TSS) with a black arrow. *Pura* enhancers (purple) were fused with the *Pura* basal promoter (-50bp to +50bp of TSS, yellow) to drive Tomato expression. This map shows the enhancer used in the original 2kb *Pura-Tomato A* reporter, the 1.5kb *Pura-Tomato B* enhancer that lacks the 5'UTR, and the 116bp enhancer in *Pura-Tomato P.*

(B) *Pura-Tomato A* and *Pura-Tomato P* have similar phase rhythms in larval LN_vs. Transgenic larvae with either *Pura-Tomato A* (black line in graph) or *Pura-Tomato P* (purple) were entrained in LD cycles at 25°C and brains dissected at the times shown. Staining, quantification and normalization are as in Fig. 1B with data from ZT0 replotted at ZT24. *Pura-Tomato A* and *P* levels vary with time in LN_vs (one-way ANOVA, $p < 0.0001$). Error bars show SEM. The graph is an average of 2 independent experiments with 15-20 LN_vs from 5 brains in each experiment.

(C) *Pura-Tomato A* and *Pura-Tomato P* respond similarly to neuronal activity. Larvae with *Pdf-Gal4* expressing *UAS-Kir2.1* (*Kir2.1*, blue), *UAS-GFP* (*GFP*, black) or *UAS-NaChBac* (*NCB*, red) and either *Pura-Tomato A* or *Pura-Tomato P* were entrained in LD cycles. Larval brains were dissected at ZT12, stained, quantified and the data normalized as in Fig. 1B.
Left: *Pura-Tomato A* levels are higher in *Kir2.1*-expressing LN_vs and lower in *NCB*-expressing LN_vs than in *GFP*-expressing LN_vs (Student's *t*-test, *Kir2.1* vs *GFP* $p < 0.0001$, *NCB* vs *GFP* $p < 0.05$).
Right: *Pura-Tomato P* levels are higher in *Kir2.1*-expressing LN_vs and lower in *NCB*-expressing LN_vs than in *GFP*-expressing LN_vs (Student's *t*-test, *Kir2.1* vs *GFP* $p < 0.0001$, *NCB* vs *GFP* $p < 0.01$). Error bars show SEM. The graph shows an average of 2 independent experiments with 15-20 LN_vs from 5 brains in each experiment.

(D) cis-regulatory elements in *Pura enhancer P*. The DNA sequence of the 116bp *Pura enhancer P* along with predicted binding sites for potential activators (Pax6 and E for E-box) in blue above the DNA sequence and potential repressors (Atf3, Egr-1 and Mef2) in red below the DNA sequence.

(E) *Pura-Tomato P* is repressed by Mef2, Sr and Atf3. *Pura-Tomato P* levels were measured in LN_vs at ZT12 from larvae with *Pdf-Gal4* expressing *UAS-Dcr-2* and a UAS transgene to either overexpress Mef2, Sr or Atf3 or an RNAi transgene to reduce expression. *UAS-GFP* (*GFP*) was used as a control. Larval brains were dissected, stained, quantified and the data normalized as in Fig. 1B.
Left: *Pura-Tomato P* levels are lower in LN_vs over-expressing *Mef2* (*Pdf* > *Mef2*) and higher in *Mef2-RNAi*-expressing LN_vs (*Pdf* > *Mef2-RNAi*) than in control LN_vs (*Pdf* > *GFP*). Student's *t*-test: *Pdf* > *Mef2* vs *Pdf* > *GFP*, $p < 0.001$; *Pdf* > *Mef2-RNAi* vs *Pdf* > *GFP*, $p < 0.0001$.

Middle: *Pura-Tomato P* levels are lower in LN_vs over-expressing *sr* (*Pdf* > *sr*) and higher in *sr-shRNA*-expressing LN_vs (*Pdf* > *sr-shRNA*) than in control LN_vs (*Pdf* > *GFP*). Student's *t*-test: *Pdf* > *sr* vs *Pdf* > *GFP* and *Pdf* > *sr-shRNA* vs *Pdf* > *GFP*, $p < 0.0001$. Right: *Pura-Tomato P* levels are lower in LN_vs over-expressing *Atf3* (*Pdf* > *Atf3*) and higher in *Atf3-RNAi*-expressing LN_vs (*Pdf* > *Atf3-RNAi*) than in control LN_vs (*Pdf* > *GFP*). Student's *t*-test: *Pdf* > *Atf3* vs *Pdf* > *GFP* and *Pdf* > *Atf3-RNAi* vs *Pdf* > *GFP*, $p < 0.0001$. Error bars show SEM. The graphs show an average of 2 independent experiments with 15-20 LN_vs from 5 brains in each experiment.

(F) An E-box in *Pura enhancer P* is important for expression in LN_vs. Larvae with either wild type *Pura-Tomato P* or with the core of the E-box mutated (*Pura-Tomato P mE*) were entrained in LD cycles at 25°C. Larval brains were dissected at ZT12 and stained, quantified and the data normalized as in Fig. 1B. *Pura-Tomato P* levels (black) in LN_vs are higher than *Pura-Tomato P mE* (grey, Student's *t*-test, $p < 0.0001$). The graph is an average of 2 independent experiments with 15-20 LN_vs from 5 brains in each experiment.

(G) The E-box in the minimal *Pura* enhancer is not required for transcriptional activation by Kir2.1. *Pura-Tomato P mE* levels were measured in LN_vs at ZT12 from larvae with *Pdf-Gal4* expressing either *UAS-GFP* (*Pdf* > *GFP*, grey) or *UAS-Kir2.1* (*Pdf* > *Kir2.1*, blue). Larval brains were dissected, stained, quantified and the data normalized as in Fig. 1B. *Pura-Tomato P mE* levels are higher in *Kir2.1*-expressing LN_vs than in control LN_vs (Student's *t*-test, $p < 0.0001$). Error bars show SEM. The graph is an average of 2 independent experiments with 15-20 LN_vs from 5 brains in each experiment.

Figure 5. Toy is a hyperpolarization-induced activator of *Pura*.

(A) An RNAi screen identified the transcription factor Toy as an activator of *Pura*. Larvae with *Pura-Tomato B*, *Pdf-Gal4*, *UAS-Dcr-2* and one of 110 *UAS-transcription factor-shRNA* transgenes or a control transgene *UAS-GFP* (*GFP*) were entrained in LD cycles at 25°C. Larval brains were dissected at ZT18 and stained and quantified as in Fig. 1B. Tomato signals in single LN_vs were normalized to the mean of the *GFP*-expressing control LN_vs. Each grey bar represents the average *Pura-Tomato B* levels in 10-16 LN_vs from 4 brains with one *UAS-transcription factor-shRNA* transgene. Error bars show SEM. Dashed lines show the mean of *Pura-Tomato B* levels in control LN_vs ± 2

S.D. The lowest levels of *Pura-Tomato B* were in *UAS-toy-shRNA* expressing LN_vs (Student's *t*-test, $p < 0.0001$ vs control LN_vs).

(B) The minimal *Pura* enhancer is activated by Toy. *Pura-Tomato P* levels were measured at ZT12 in larvae with *Pdf-Gal4* expressing *UAS-Dcr-2* and a control *UAS-GFP* transgene (*Pdf > GFP*, black) overexpressing *toy* via *UAS-toy* (*Pdf > toy*), or reducing *toy* expression via *UAS-toy-shRNA* or *UAS-toy-RNAi* transgenes (*Pdf > toy-shRNA* and *Pdf > toy-RNAi*, blue). Larval brains were dissected, stained, quantified and the data normalized as in Fig. 1B. *Pura-Tomato P* levels are higher in *Pdf > toy* LN_vs and lower with either *toy-shRNA* or *toy-RNAi* expressed in control LN_vs (Student's *t*-test, $p < 0.0001$ for *Pdf > toy-shRNA* vs *Pdf > GFP* and *Pdf > toy-RNAi* vs *Pdf > GFP*). Error bars show SEM. The graph is an average of 2 independent experiments with 15-20 LN_vs from 5 brains in each experiment.

(C) The predicted Toy binding site in *Pura P* is required for expression in LN_vs. Larvae with *Pura-Tomato P* (black) or with the Toy binding site mutated (*Pura-Tomato P mT*, grey) were entrained in LD cycles. Larval brains were dissected at ZT12 and stained as in Fig. 1B. Tomato signals in single LN_vs were quantified and normalized to the average of the signals from *Pura-Tomato P* LN_vs. *Pura-Tomato P* levels in LN_vs are higher than *Pura-Tomato P mT* (Student's *t*-test, $p < 0.0001$). The graph shows an average of 2 independent experiments with 15-20 LN_vs from 5 brains in each experiment.

(D) Rhythms in Toy protein levels in LN_vs. Wild type larvae were entrained in LD cycles at 25°C, dissected at the times shown and stained with antibodies to Toy (purple) and PDF to mark LN_vs (blue).
Top: Representative confocal images from ZT12 and ZT18. Single channel images show Toy signals in grayscale with dashed lines circling the areas quantified.
Bottom: Toy signals in LN_vs were quantified, normalized to the average of the peak time point and plotted. Data from ZT0 are replotted at ZT24. Error bars show SEM. Toy protein levels vary with time (one-way ANOVA, $p < 0.0001$). The graph is an average of 2 independent experiments with 15-20 LN_vs from 5 brains in each experiment.

(E) Toy protein levels in LN_vs are regulated by altered electrical activity. Toy levels were measured at ZT12 in LN_vs from larvae with *Pdf-Gal4* expressing either *UAS-GFP*

as control (*Pdf* > *GFP*, black) or *UAS-NaChBac* (*Pdf* > *NCB*, red) or *UAS-Kir2.1* (*Pdf* > *Kir2.1*, blue). Toy levels were quantified and normalized as in Fig. 5D.
Top: representative confocal images are shown with Toy protein in purple and PDF in blue. Single channel images with Toy signals in grayscale are shown with dashed lines circling the areas quantified.
Bottom: Toy protein levels are higher in *Pdf* > *Kir2.1* LN_vs and lower in *Pdf* > *NCB* LN_vs than control *Pdf* > *GFP* LN_vs (Student's *t*-test, *Pdf* > *Kir2.1* vs *Pdf* > *GFP* $p < 0.0001$; *Pdf* > *NCB* vs *Pdf* > *GFP*, $p < 0.05$). Error bars show SEM. The graph is an average of 2 independent experiments with 15-20 LN_vs from 5 brains in each experiment.

(F) *toy* transcription is rhythmic in LN_vs. Larvae with a *toy-Tomato* reporter gene were dissected at different times of day, stained, quantified and normalized as in Fig. 1B.
Top: representative confocal images at ZT12 and ZT18.
Bottom: *toy-Tomato* levels plotted against time with data from ZT0 replotted at ZT24. Error bars show SEM. *toy-Tomato* levels vary with time in larval LN_vs (one-way ANOVA, $p < 0.0001$). The graph is an average of 2 independent experiments with 15-20 LN_vs from 5 brains in each experiment.

(G) *toy* transcription is activated by hyperpolarization. *toy-Tomato* levels were measured in LN_vs from larvae with *Pdf-Gal4* expressing *UAS-Kir2.1* (*Pdf* > *Kir2.1*, blue), *UAS-GFP* (*Pdf* > *GFP*, black), or *UAS-NaChBac* (*Pdf* > *NCB*, red). Larval brains were dissected at ZT12, stained, quantified and the data normalized as in Fig. 1C.
Top: representative confocal images with Tomato (red) and PDF (blue) to mark LN_vs.
Bottom: *toy-Tomato* levels are higher in *Pdf* > *Kir2.1*-expressing LN_vs than in control *Pdf* > *GFP* LN_vs (Student's *t*-test, $p < 0.0001$). There is no difference in *toy-Tomato* levels between *Pdf* > *NCB* and control LN_vs (Student's *t*-test, $p > 0.05$). Error bars show SEM. The graph is an average of 2 independent experiments with 15-20 LN_vs from 5 brains in each experiment.

Figure 6. A model for how *Pura* responds to neuronal activity
Neuronal activity activates Mef2 to repress *Pura* transcription. Neuronal activity also induces *Atf3* and *sr* transcription and Atf3 and Sr proteins also repress *Pura*. Hyperpolarization induces *toy* transcription and Toy protein then activates transcription of *Pura*. The Toy binding site overlaps with Sr and Mef2 binding sites in the minimal *Pura enhancer*.

Methods

1. Cloning strategies:

We modified pBPGUw (Pfeiffer et al., 2008), Addgene) to create a vector to make fluorescent reporter genes for different enhancers. pBPGUw contains a Gateway cassette to easily insert enhancers through the LR reaction upstream of the synthetic basal promoter DSCP. pBPGUw also contains a *PhiC31 attB* sequence for site-specific genome insertion and a mini *white*$^{+}$ gene to select transformants. We PCR-amplified DNA for codon-optimized *tdTomato*, 3 copies of nuclear localization sequence, a *PEST* sequence and a *SV40* 3'UTR (Mezan et al., 2016). PCR products were TOPO cloned to the pCRXL-TOPO vector (Life Technologies)**,** digested out with KpnI and SpeI. This insert was ligated to KpnI / SpeI-digested pBPGUw which removes the *Gal4* sequence. We called the resulting plasmid pZT.

Since Pfeiffer et al. (Pfeiffer et al., 2010) and our preliminary data showed that the *DSCP* basal promoter is relatively weak, we replaced *DSCP* with the *Hsp70* basal promoter. We also added an intervening sequence (IVS) and a synthetic 5'UTR (*Syn21*) to increase translational efficiency as in (Pfeiffer et al., 2010; Pfeiffer et al., 2012). Since there were no restriction sites available for direct cloning, a DNA fragment containing the Hsp70 basal promoter, IVS, *Syn21* 5'UTR and part of tdTomato cDNA was synthesized by Integrated DNA Technologies using the sequences from (Pfeiffer et al., 2010; Pfeiffer et al., 2012). This DNA fragment was flanked by FseI and SbfI sites. The fragment was amplified by PCR, TOPO cloned to pCR8GWTOPO, and digested by FseI and SbfI to remove it from the vector. This fragment was inserted into pZT digested with FseI and SbfI to create pZT2.0. The DNA sequence was verified by Sanger sequencing (Genewiz).

For *Hr38-Tomato*, we used PCR to amplify the 4kb of *Hr38* regulatory DNA in *Hr38*^{GMR36B12}*-Gal4* (Jenett et al., 2012) from fly genomic DNA. This DNA was TOPO cloned to pCR8GWTOPO vector to create pCR8GWTOPO-*Hr38 enhancer*. Then we performed an LR reaction (Gateway™ LR Clonase™ II Enzyme mix, Thermo Scientific) to insert the *Hr38* enhancer into pZT2.0 to make *Hr38-Tomato*.

For *Hr38-GFP*, we modified pZT2.0 by replacing the tdTomato sequence with a codon optimized *GFP* (Lee and Luo, 1999). We used PCR to amplify *GFP* from pJFRC81-10XUAS-IVS-Syn21-GFP-p10 (JFRC, Addgene) and added an AgeI site to the reverse primer. The PCR products were TOPO cloned to pCR8GWTOPO vector. The resulting

plasmid was digested with KpnI and AgeI and inserted into pZT2.0 digested with KpnI and AgeI to remove *tdTomato* sequences. The resulting plasmid (pZT2.5) contains the same elements as pZT2.0 except *GFP* instead of *tdTomato*. Then we used an LR reaction to insert 4kb of *Hr38* regulatory DNA from pCR8GWTOPO-*Hr38 enhancer* to pZT2.5 to create *Hr38-GFP*.

All *Pura-Tomato* transgenes were driven by an endogenous *Pura* basal promoter (-50bp to +50bp of the transcription start site of *Pura* isoform B). We modified pZT2.0 to either remove the HSP70 basal promoter (pZT2.3) or replace it with the *Pura* basal promoter (pZT2.4). To make pZT2.3, we digested pZT2.0 with FseI and BglII and ligated a 22bp synthetic fragment with FseI and BglII sticky ends. Then we used PCR to amplify the *Pura* enhancers A, B, B1, B2, C, D and E from fly genomic DNA. These fragments contained the *Pura* basal promoter. They were cloned into pCR8GWTOPO and LR reactions were used to insert these enhancers into pZT2.3 to generate *Pura-Tomato* transgenes.

pZT2.4 contains the *Pura* basal promoter in the backbone. We synthesized an 114bp fragment containing the *Pura* basal promoter with an FseI site and a BglII site on the 5'end and 3' end respectively. We cloned the 114bp basal promoter fragment into pCR8GWTOPO and cut with FseI and BglII to make the insertion. We also cut pZT2.0 with FseI and BglII to create the backbone and ligated it with the *Pura* basal promoter insertion. This generated plasmid pZT2.4. We used PCR to amplify *Pura* enhancer fragments F, G, H, I, J, K, L, M, N and P from fly genomic DNA, which do not include the *Pura* basal promoter. Then we used TOPO cloning to insert each one to pCR8GWTOPO and used LR reactions to insert these enhancers into pZT2.4 to generate *Pura-Tomato* transgenes.

To make *Pura-Tomato P mE*, we changed the E-box sequence CACGTG in *Pura enhancer P* to CA**GC**TG (mutations in bold) according to (Darlington et al., 1998) and synthesized the mutated 116bp DNA sequence (Integrated DNA Technologies). We cloned the synthesized DNA fragment into the pCR8GWTOPO vector to create pCR8GWTOPO-*Pura enhancer P mE* and then performed an LR reaction to insert *Pura enhancer P mE* to pZT2.4 to generate *Pura-Tomato P mE*.
To make Pura-Tomato PmT, we mutated the sequence TCTACTGGGCACGCACGC in *Pura enhancer P* that contains the Toy binding site to T**T**T**C**C**G**G**A**G**T**A**T**G**T**A**T**G**T** (mutations in bold) and synthesized the mutated 116bp DNA sequence (Integrated DNA

Technologies). We cloned the synthesized DNA fragment into the pCR8GWTOPO vector to create pCR8GWTOPO-*Pura enhancer P mT* and then performed an LR reaction to insert *Pura enhancer P mT* to pZT2.4 to generate *Pura-Tomato P mT*.

For *toy-Tomato*, we used PCR to amplify a 3.6kb *toy enhancer* DNA fragment from fly genomic DNA and cloned it into the pCR8GWTOPO vector to create pCR8GWTOPO-*toy enhancer*. Then we performed an LR reaction to insert the *toy enhancer* to pZT2.0 to make *toy-Tomato*.

For *4X CRE-Tomato*, a 143bp DNA fragment containing 4 copies of a canonical CRE element (Integrated DNA Technologies) using a sequence provided by Dr. Subhabrata Sanyal was cloned into the pCR8GWTOPO vector to create pCR8GWTOPO-4X CRE. We then performed an LR reaction to insert the synthetic 4X CRE sequence to pZT to make *4X CRE-Tomato*.

2. Generating transgenic animals

All plasmids containing reporter transgenes were prepared using Qiagen Plasmid Mini Kit (Qiagen Ref No.12125). The plasmids were sent to Genetivision Corporation for injection. All reporter transgenes were inserted to a specific site using PhiC31 recombinase mediated methods (Groth et al., 2004). All transgenes were inserted to VK37: (2L)22A3 (Venken et al., 2006) except for *Hr38-GFP* which was inserted to attP2: (3L)68A4 (Groth et al., 2004). Since all of the transgenes contain a mini *white*$^+$ selection marker, plasmids were injected to *white* loss-of-function mutant flies to make transgenic lines and crossed to *white* loss-of-function mutant flies to screen for *white*$^+$ transgenic flies. Red eyed flies were balanced to make stock lines.

3. Immunofluorescence staining

Flies were developed at 25°C in LD cycles unless specifically noted. Brains of *Drosophila* 3rd instar wandering larvae were dissected at specific times of day in phosphate-buffered saline (PBS) and immediately fixed in fresh 4% formaldehyde in PBS for 20 min at room temperature. Brains were then permeabilized by washing twice in PBS with 1% Triton X-100 for 10 min and then blocked in PBS with 0.5% Triton X-100 and 10% normal horse serum (VECTOR S-2000) for at least 30 min at room temperature. Brains were incubated in PBS with 0.5% Triton X-100 and 10% normal horse serum and primary antibodies overnight at 4°C. Brains were rinsed once and then

washed 10 min for 3 times in PBS with 0.5% Triton X-100 before incubating with secondary antibodies in PBS with 0.5% Triton X-100 and 10% normal horse serum either at room temperature for 1 hr or overnight at 4°C. Brains were rinsed once and then washed 10 min for 3 times in PBS with 0.5% Triton X-100. Brains were soaked in 50% glycerol in PBS or SlowFade Gold antifade reagent (Invitrogen S36936) for 20 min before mounting.

Antibody list:
Primary antibodies:
PDF: “PDF C7”, Developmental Studies Hybridoma Bank, mouse, used at 1:100
RFP: “PM005”, MBL, rabbit, used at 1:500
Toy: gift from Claude Desplan, previously unpublished, rabbit, used at 1:500
GFP: “NB100-62622”, Novus Biologicals, sheep, used at 1:500

Secondary antibodies:
Alexa Fluro 488 donkey anti mouse (Life Technologies, A21202)
Alexa Fluro 488 donkey anti sheep (Life Technologies, A11015)
Alexa Fluro 555 donkey anti rabbit (Life Technologies, A31572)
Alexa Fluro 647 donkey anti rabbit (Life Technologies, A31573)
Alexa Fluro 647 donkey anti mouse (Life Technologies, A31571)
All used at 1:500.

4. Confocal Microscopy and Image Analysis

Brains were scanned as single stack images with 1μM in depth (1024 X 1024 or 1024 X 256 resolution) under the 20X objective lens of Leica SP5 confocal microscope with 2X or 4X digital zoom in. For quantification, a stack of images (usually 10-13 images) was projected together on the Z-axis. Mean fluorescence intensity in the soma of single neurons were quantified using FIJI with background subtracted. Background levels were determined by the average of mean fluorescence intensity of 10 regions with the same size randomly selected in the same brain lobe.

5. Bioinformatics analysis to search for transcription factor binding sites

We first used JASPAR CORE Vertebrata [jaspar.genereg.net, (Mathelier et al., 2016)] with default settings to predict CREB and Mef2 binding sites in the *Hr38* and *Pura*

enhancers. We chose the database of vertebrate transcription factors binding sites because it includes more transcription factors (1045 for vertebrates vs 266 for insects). Then we used MATCH analysis from TRANSFAC (Kel et al., 2003) with default settings to identify potential CREB, Mef2, Egr1, Atf3 and Pax6 binding sites as well as E-boxes. We used the vertebrate transcription factor PWMs for the same reason as above. In addition, the vertebrate transcription factor PWM database is better annotated for Pax6 as it includes the Paired domain binding sequence as well as the Homeodomain binding sequence – in contrast, the insect PMW only has the Homeodomain binding sequence.

6. Conservation analysis

We used the bioinformatics tool phastCons analysis in the UCSC genome browser (Siepel et al., 2005) to identify the DNA sequences in the *Pura enhancer P* that are conserved in *D. pseudoobscura* and *D. virilis*. Then we used MATCH analysis to predict transcription factor binding sites in these regions in *D. pseudoobscura* and *D. virilis* as above.

7. Statistics

All data points were normalized to the mean of the control group unless specified in figure legends. Error bars in all figures show mean ± SEM. Sample size (n) of all experiments is indicated in figure legends. All experiments with LN_vs measured at least 15-20 single cells from 5 individual brains were quantified in each of 2 independent experiments. Student's t test was used to test for significant difference ($p < 0.05$) vs. control groups in most experiments. One-way ANOVA was performed to determine significant difference ($p < 0.05$) for rhythmic expression levels.

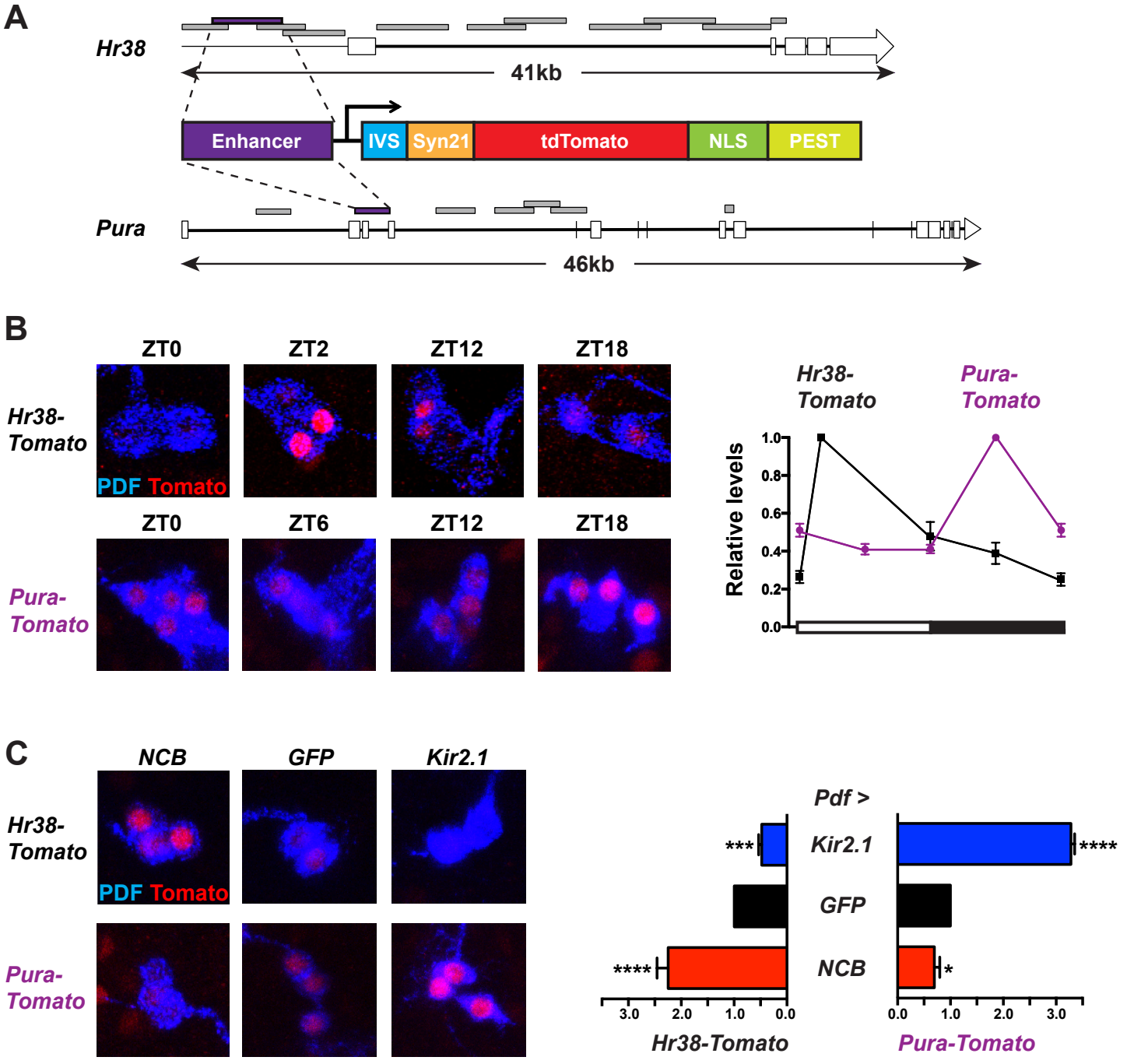

Zhu et al. Figure 1

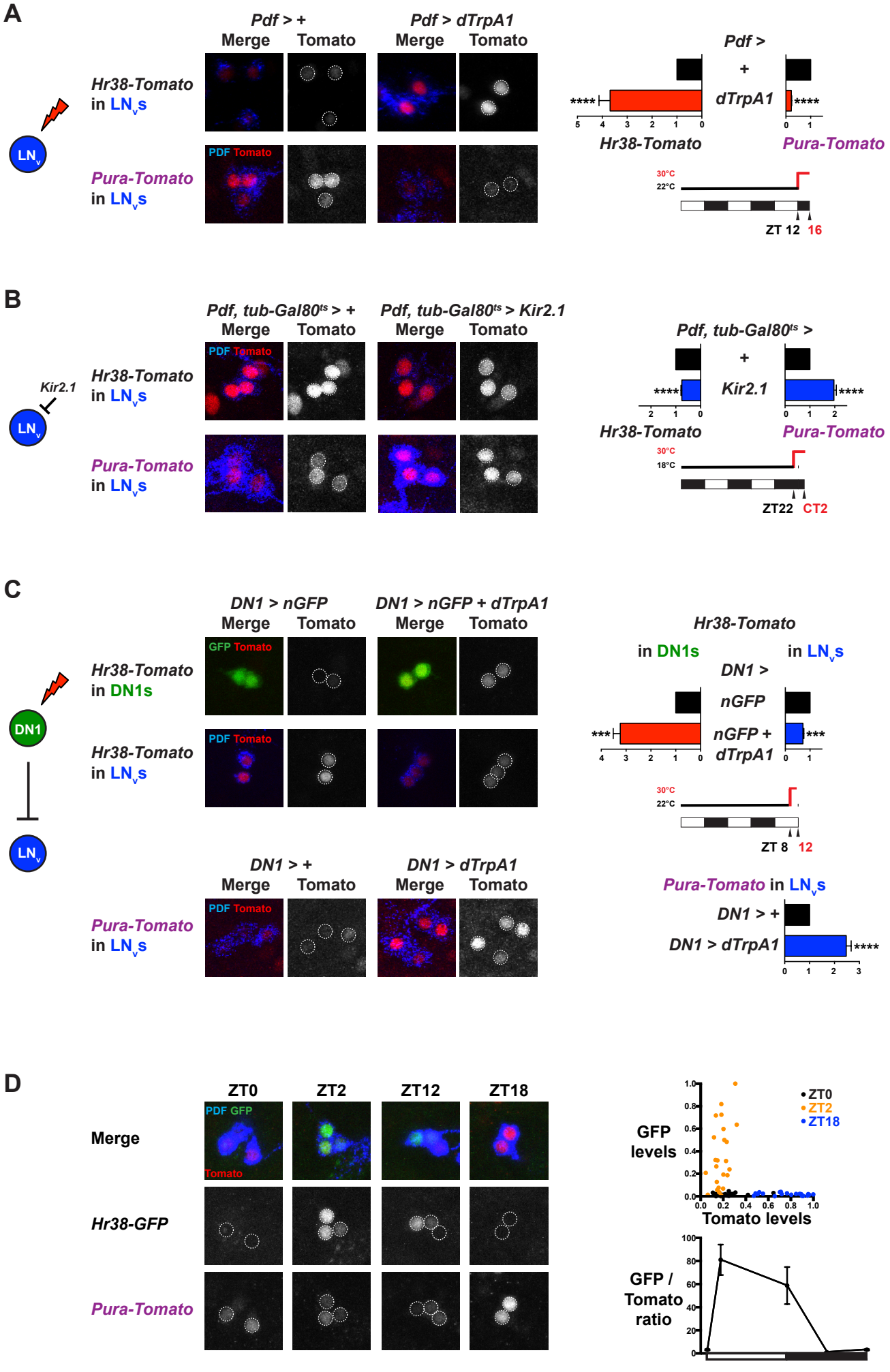

Zhu et al. Figure 2

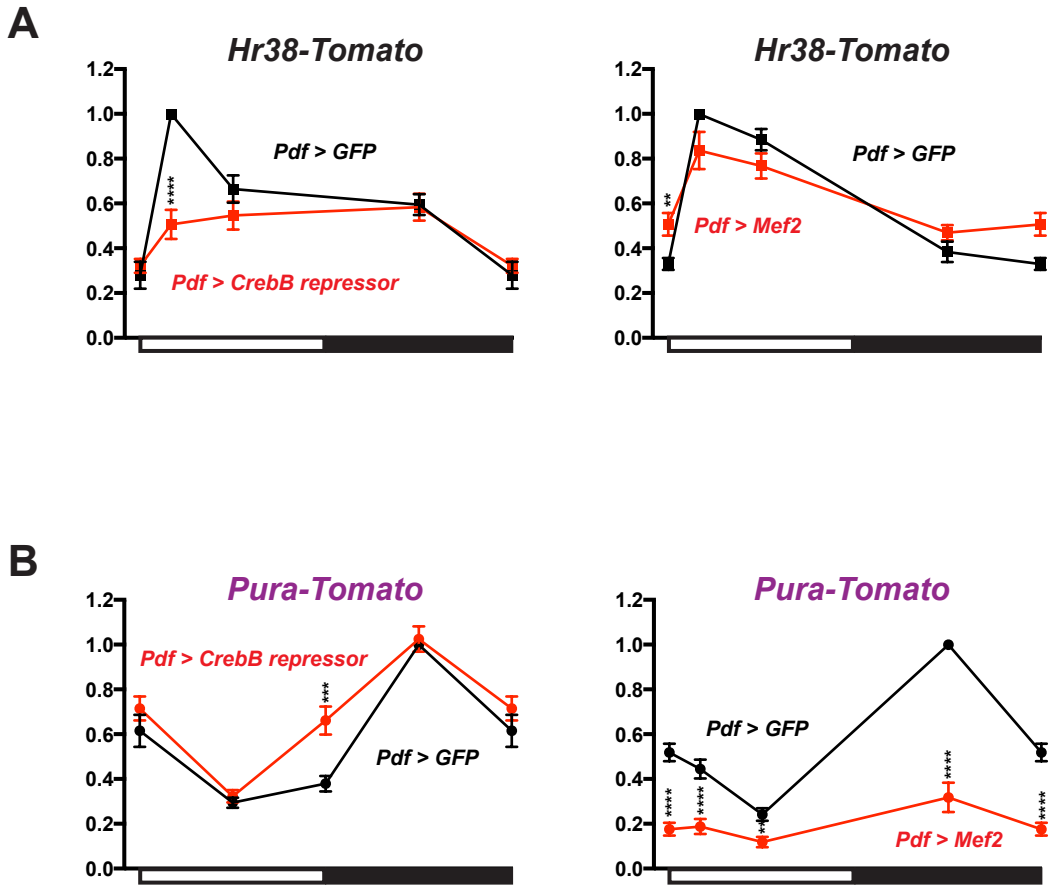

Zhu et al. Figure 3

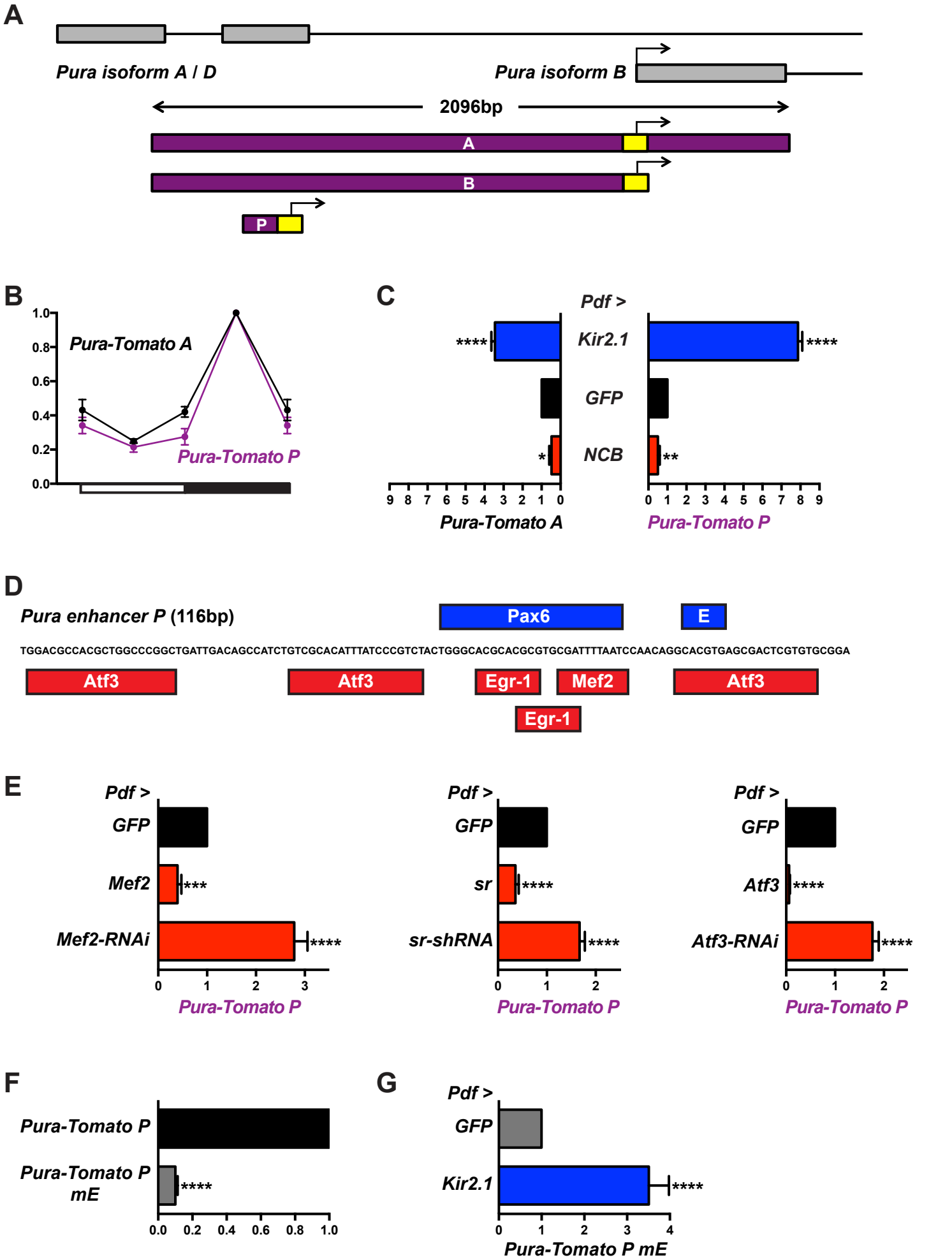

Zhu et al. Figure 4

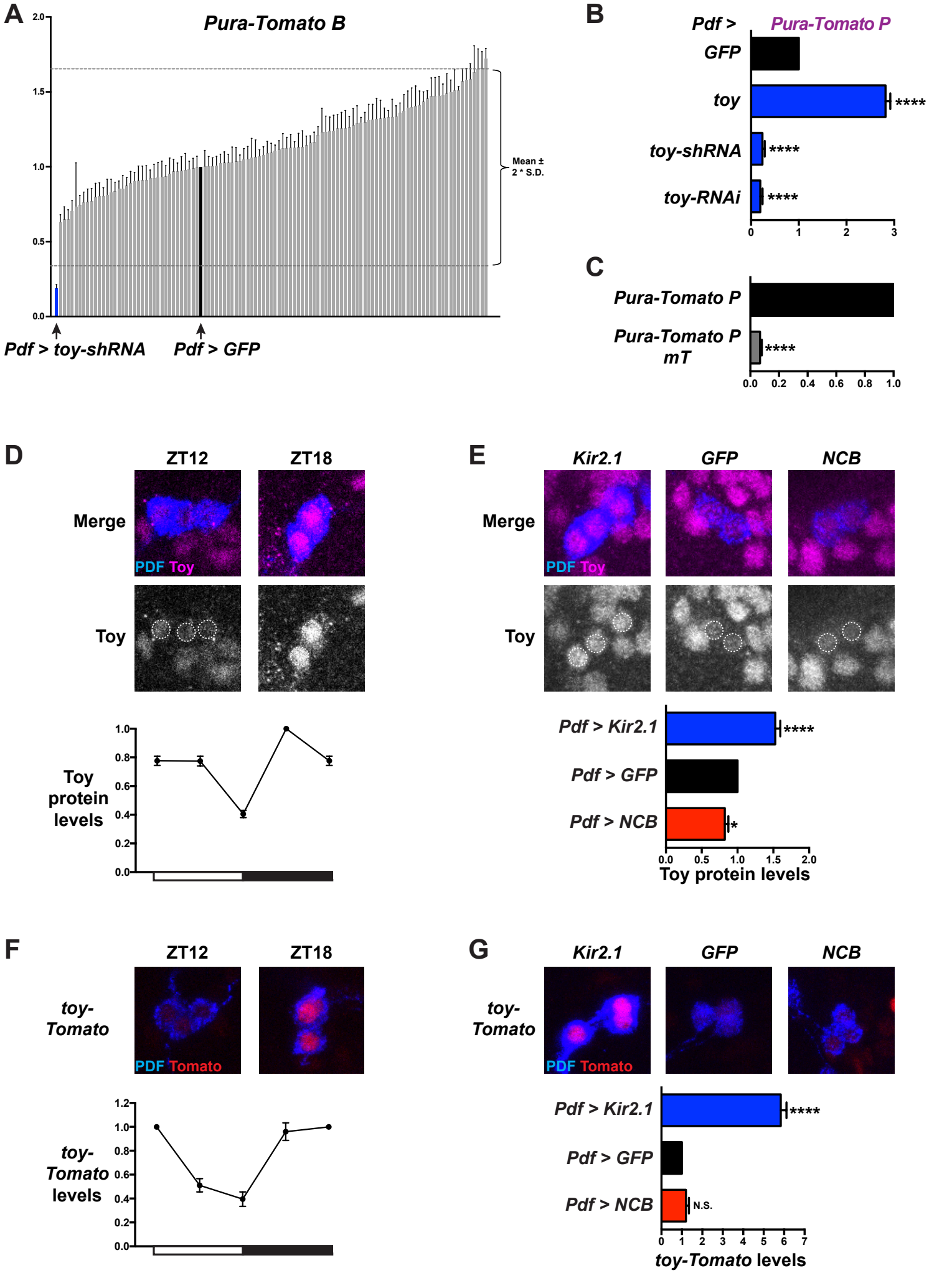

Zhu et al. Figure 5

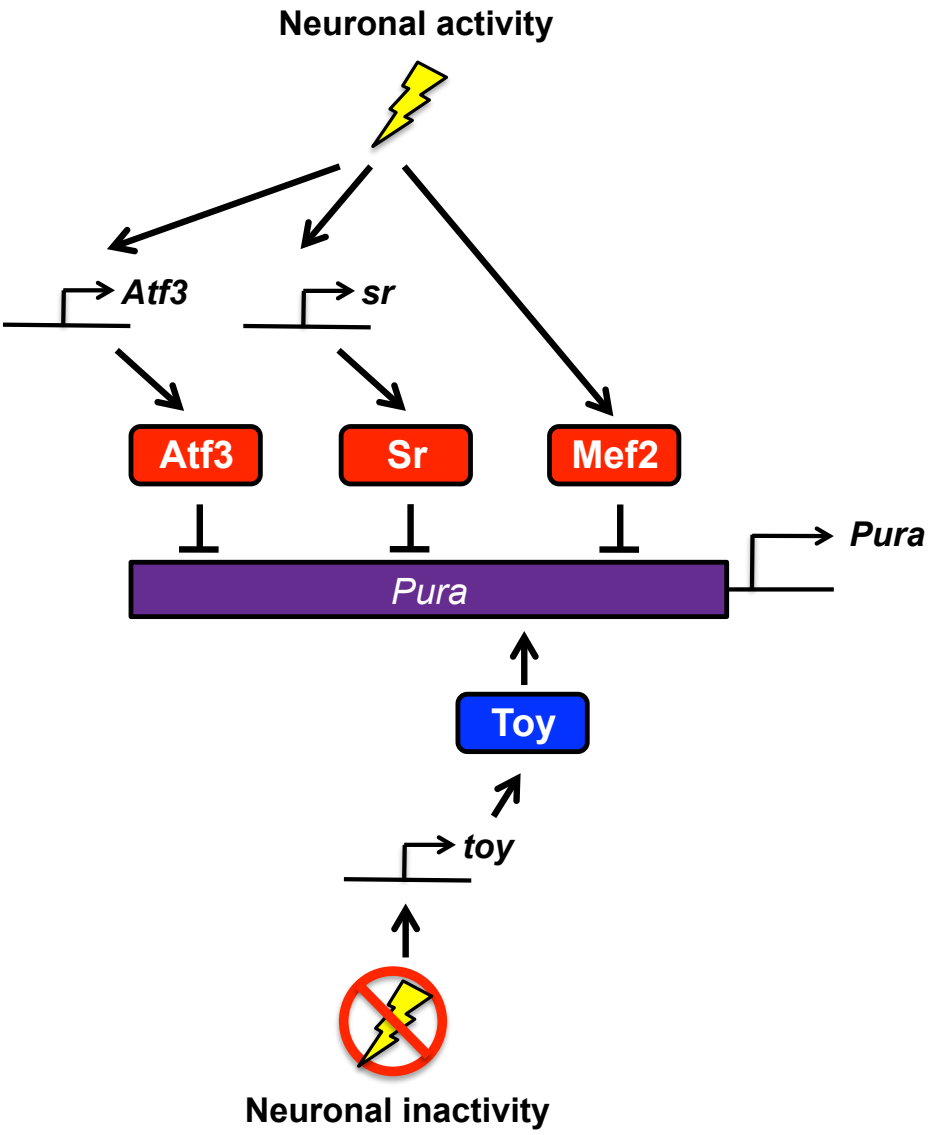

Zhu et al. Figure 6